Upwelling of deep mantle material through a plate window: Evidence from the geochemistry of Italian basaltic volcanics

D. Gasperini,[1,2] J. Blichert-Toft,[1] D. Bosch,[3] A. Del Moro,[4] P. Macera,[2] and F. Albarède[1]

Received 2 February 2001; revised 30 March 2002; accepted 2 April 2002; published 26 December 2002.

[1] The isotopic compositions of basaltic lavas from the Quaternary and Plio-Pleistocene Italian volcanics (Tuscan Magmatic Province, Roman Magmatic Province, Vesuvius, Aeolian Islands, Etna, and Iblean Basin) define binary hyperbolic relationships in the $^{87}Sr/^{86}Sr-^{206}Pb/^{204}Pb-\varepsilon_{Nd}-\varepsilon_{Hf}$ space. The isotopic compositions of the two end-members of these mixing arrays are assessed by least-squares regression. The mantle-derived component ($^{206}Pb/^{204}Pb = 19.8$, $^{87}Sr/^{86}Sr = 0.7025$, $\varepsilon_{Nd} = +8$, $\varepsilon_{Hf} = +9$) is a rather homogeneous mixture of the standard high-μ (HIMU) and depleted mantle (DM) components. The crust-derived component ($^{206}Pb/^{204}Pb = 18.5$, $^{87}Sr/^{86}Sr > 0.715$, $\varepsilon_{Nd} = -12$, $\varepsilon_{Hf} = -11$) accounts for the enrichment of K and other large-ion-lithophile elements in the Italian volcanics. As shown by the relationship in $\varepsilon_{Hf}-\varepsilon_{Nd}$ space and the lower-than-chondritic Hf/Sm ratio, this crustal component is dominated by pelagic sediments rather than terrigenous material. The overall scarcity of calc-alkaline compositions in the Italian volcanics and the presence of a HIMU component, which is the hallmark of hot spot basalts, raise the question of how plume mantle source contributes to volcanism in a subduction environment. At about 13 Ma, the Apennine collision terminated the westward subduction of the Adria plate under the European margin and rotated the direction of convergence to the northwest. The cumulative differential of subduction between the fossil plate under Tuscany and the active plate under Sicily since the opening of the Tyrrhenian Sea amounts to at least 300 km and is large enough to rift the dipping plate and open a plate window beneath the southern part of the peninsula. This model is consistent with recent high-resolution seismic tomography. We propose that the counterflow of mixed upper and lower mantle passing the trailing edge of the rifted plate is the source of Italian mafic volcanism. Alternatively, material from a so-far unidentified plume may be channeled through the plate window. The crustal signature is probably acquired by interaction of the mantle advected through the window with the upper part of the subducted plate. *INDEX TERMS:* 1749 History of Geophysics: Volcanology, geochemistry, and petrology; 1025 Geochemistry: Composition of the mantle; 1040 Geochemistry: Isotopic composition/chemistry; *KEYWORDS:* Italian volcanism, HIMU, subduction, pelagic sediments, mixing, slab window

Citation: Gasperini, D., J. Blichert-Toft, D. Bosch, A. Del Moro, P. Macera, and F. Albarède, Upwelling of deep mantle material through a plate window: Evidence from the geochemistry of Italian basaltic volcanics, *J. Geophys. Res.*, *107*(B12), 2367, doi:10.1029/2001JB000418, 2002.

1. Introduction

[2] Italian volcanics offer the unusual scenario of a well-characterized subduction zone environment fringed by dominantly non-calc-alkaline magmatism. Although felsic magmas interpreted as produced by melting of the continental crust are erupted locally, especially in the Tuscan area [*Hawkesworth and Vollmer*, 1979; *Marinelli and Mittempergher*, 1966], the major active volcanoes (Etna, Vesuvius, Stromboli) and the recent volcanic centers in the Roman region erupt basaltic lavas with plume affinity [*Hamelin et al.*, 1979; *Vollmer*, 1976]. *Morris and Hart* [1983] were the first to speculate on how mantle with ocean–island basalt (OIB) geochemical affinity transfer through subducting plates and proposed the "plum-pudding" model of mantle heterogeneity distribution. Because of a long history of detailed geological and geochemical studies, the Italian volcanic region is one of the best localities in which to address this issue. In addition, many of these volcanics are known for their extreme K enrichment (up to 8 wt.% K_2O in basalts from the Roman Magmatic Province) and a strong overall enrichment in incompatible elements. This enrichment has been ascribed to a variety of processes such as

[1]Ecole Normale Supérieure, Lyon, France.
[2]Dipartimento di Scienze della Terra, Universita' degli Studi di Pisa, Pisa, Italy.
[3]Laboratoire Tectonophysique, UMR-CNRS 5568, Université Montpellier 2, Montpellier, France.
[4]Istituto di Geoscienze e Georisorse, CNR, Pisa, Italy.

0148-0227/02/2001JB000418$09.00

mantle metasomatism with [*Civetta et al.*, 1981; *Thompson*, 1977; *Vollmer and Hawkesworth*, 1980] or without [*Cundari*, 1980] dehydration of the subducting plate, modification of the mantle source by sediments scraped off the subducting plate [*Ellam et al.*, 1989; *Peccerillo and Manetti*, 1985; *Rogers et al.*, 1985], and interaction of mantle melts with the overlying continental crust [*Vollmer*, 1976]. Because the enrichment of incompatible elements in Italian mafic volcanics is extreme, these rocks are ideally suited for the investigation of shallow-level interaction of mantle-derived magmas with the slab, the overlying mantle wedge, and the continental crust.

[3] This work presents new Sr, Nd, Hf, and Pb isotope data for relatively undifferentiated basaltic lavas from the Tuscan Magmatic Province (TMP) in the north through the Roman Magmatic Province (RMP) and Vesuvius in the center to the Aeolian Islands and Etna in the south. We also report major and trace element data for the same samples. Finally, these data are complemented with measurements of a few samples from the basaltic basement of the Tyrrhenian Sea (Leg 107). This new data set reveals remarkably smooth mixing relationships among all the samples from the Italian peninsula and Sicily. We use the pronounced OIB-type isotope characteristics of most of the mafic magmas present in this area to argue for a new model in which vertical mixing across a slab window allows the eruption of plume-type magmas in a subduction environment.

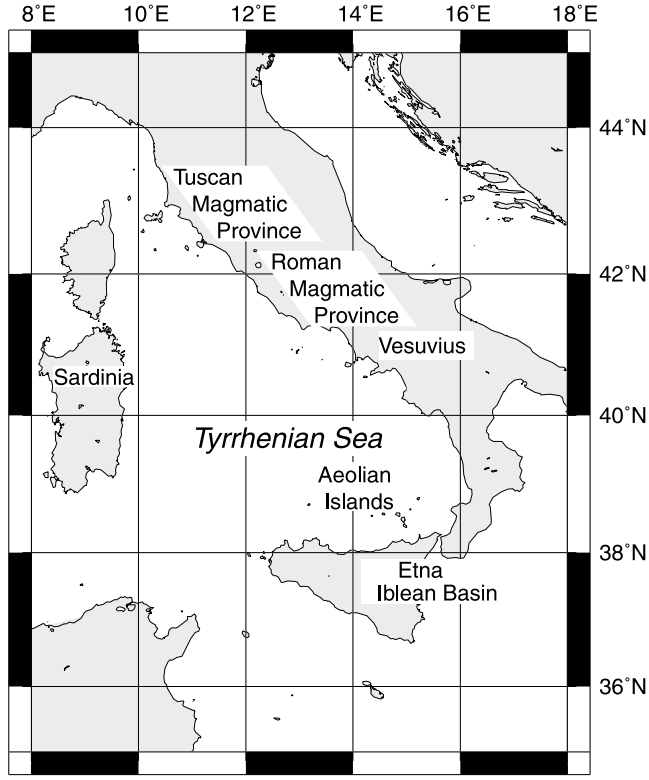

Figure 1. Sketch map showing locations of samples analyzed in this work.

2. Sample Selection

[4] A detailed geological outline is given in Appendix A. Fifteen Pleistocene mafic potassic and ultrapotassic rocks from different volcanic centers of the RMP (Vulsini, Sabatini, Vico, Ernici) and two similar types of samples from the TMP (Radicofani, Cimini), both regions of central Italy, as well as nineteen Quaternary rocks from southern Italy (Vesuvius, Tyrrhenian Basin, Aeolian Islands, Iblean Basin, Etna) were analyzed (Figure 1). For a few samples from the latter group, Nd, Sr, and Pb isotopes and major and trace element analyses already existed in the literature on the same powders and were not reanalyzed here. Most of the mafic samples are characterized by Mg# higher than 62 and SiO_2 contents typically lower than 52 wt.%, as well as low phenocryst abundances. A few mafic samples from the Vulsini district of the RMP (Montefiascone) and from Vico volcano (RMP) are fresh glass-bearing scorias. No cumulate rocks were included in the sample suite studied here.

3. Results

[5] Major and trace element data are reported in Table A1 (Appendix A) and Table 1 lists the Sr, Nd, Hf, and Pb isotope results.

3.1. Central Italy: TMP and RMP

[6] The composition of TMP and RMP samples range from basanites to phonotephrites and from basalts to shoshonites (Table A1). All samples are characterized by extreme enrichments in incompatible large-ion-lithophile (LIL)- and light-rare earth (LRE)-elements (Figure 2) and show comparable primitive mantle-normalized spider diagrams (Figure 2). These are characterized by (a) enrichment that decreases progressively from Rb to Lu, (b) negative anomalies of Ti, P, Ta, Nb, and Ba, and (c) positive anomalies of Rb, Th, U, and Pb. Their Ti, Ta, and Nb contents and high-field-strength-element (HFSE) to LILE ratios are markedly lower than those of other ultrapotassic suites, such as the leucitites from Leucite Hills [*Bergman*, 1987] and the alkaline rocks from the East African Rift [*Thompson et al.*, 1984], and rather resemble those of subduction-related volcanic rocks [*Hickey et al.*, 1986; *Thorpe et al.*, 1984].

[7] In Sr–Nd–Hf isotope space, all analyzed TMP and RMP samples plot within the enriched quadrant (Figures 3 and 4). Together with additional Italian volcanic data from the literature, they define relatively smooth hyperbolic relationships (Figure 3; Hf not shown due to lack of such data in the literature). The isotopic compositions of Sr, Nd, and Hf signaling the most depleted source are found at Ernici (RMP, southern Latium), whereas the most enriched samples are found at Cimini (TMP) and Vico (RMP, northern Latium). The Tuscan mafic lavas have the most radiogenic $^{87}Sr/^{86}Sr$ and the lowest $^{143}Nd/^{144}Nd$ ratios, overlapping the field of Elba granites [*Juteau et al.*, 1986]. In $\varepsilon_{Hf}-\varepsilon_{Nd}$ space (Figure 4), the compositions of the RMP and TMP samples plot above the Hf–Nd isotope mantle array, falling in the radiogenic Hf part of the continental crust field. Below, we discuss in greater detail the significance of the observation that they also plot within the field of pelagic sediments [*Vervoort et al.*, 1999; *White and Patchett*, 1984].

Table 1. Sr, Nd, Hf, and Pb Isotope Compositions for the Most Primitive Volcanic Rocks From Central and Southern Italy[a]

Sample	Locality			$^{87}Sr/^{86}Sr$	$^{143}Nd/^{144}Nd$	ε_{Nd}	$^{176}Hf/^{177}Hf$	ε_{Hf}	$^{206}Pb/^{204}Pb$	$^{207}Pb/^{204}Pb$	$^{208}Pb/^{204}Pb$
DG1	Acquaforte	Vico	RMP	0.710718 ± 6	0.512098 ± 4	−10.53	0.282543 ± 4	−8.10	18.757	15.664	39.037
							0.282536 ± 3	−8.35			
V849B	Nibbio	Vico	RMP	0.708335 ± 7	0.512218 ± 8	−8.19	0.282602 ± 3	−6.01	18.815	15.646	39.047
							0.282599 ± 4	−6.12			
V972	Nibbio	Vico	RMP	0.708185 ± 9	0.512214 ± 8	−8.27	0.282596 ± 3	−6.22	18.827	15.659	39.078
							0.282593 ± 4	−6.33			
V971	Nibbio	Vico	RMP	0.70839 ± 11	0.512215 ± 9	−8.25	0.282578 ± 4	−6.86	18.809	15.663	39.070
							0.282578 ± 3	−6.86			
VS229	Latera	Vulsini	RMP	0.710318 ± 8	0.512146 ± 11	−9.60	0.282579 ± 4	−6.84	18.717	15.656	38.994
VS230	Latera	Vulsini	RMP	0.709941 ± 22	0.512198 ± 13	−8.58	0.282604 ± 3	−5.96	18.740	15.663	39.039
VS228	Montefiascone	Vulsini	RMP	0.710198 ± 10	0.512130 ± 9	−9.91	0.282569 ± 4	−7.19	18.779	15.653	39.015
							0.282576 ± 4	−6.93			
VS224	Montefiascone	Vulsini	RMP	0.710260 ± 15	0.512132 ± 9	−9.87	0.282565 ± 4	−7.33	18.766	15.664	39.030
							0.282563 ± 4	−7.39			
V975	Montefiascone	Vulsini	RMP	0.710371 ± 9	0.512155 ± 13	−9.42	0.282637 ± 4	−4.76	18.704	15.617	38.917
							0.282640 ± 9	−4.67			
V976	Montefiascone	Vulsini	RMP	0.710084 ± 11	0.512165 ± 7	−9.23	0.282644 ± 8	−4.54	18.762	15.665	39.028
							0.282639 ± 4	−4.70			
V977	Montefiascone	Vulsini	RMP	0.710371 ± 10	0.512162 ± 7	−9.29	0.282627 ± 4	−5.11	18.753	15.658	39.024
							0.282627 ± 13	−5.11			
DMS984	Mt. Maggiore	Sabatini	RMP	0.710086 ± 13	0.512106 ± 6	−10.38	0.282562 ± 3	−7.42	18.797	15.674	39.090
							0.282561 ± 3	−7.46			
DMS983	Bracciano	Sabatini	RMP	0.710782 ± 17	0.512117 ± 9	−10.16	0.282543 ± 5	−8.09	18.754	15.657	39.018
DME981	S. Sosio	Ernici	RMP	0.706875 ± 9	0.512357 ± 9	−5.48	0.282764 ± 6	−0.28	18.939	15.674	39.103
							0.282768 ± 5	−0.14			
DME982	S. Giuliano	Ernici	RMP	0.709764 ± 16	0.512144 ± 11	−9.64	0.282590 ± 3	−6.44	18.886	15.673	39.075
							0.282602 ± 3	−6.01			
VS221	Castello	Radicofani	TMP	0.713359 ± 16	0.512180 ± 13	−8.93	0.282554 ± 3	−7.72	18.711	15.665	39.049
VS232	Cava Piagge	Cimini	TMP	0.715647 ± 14	0.512055 ± 12	−11.37	0.282446 ± 5	−11.53	18.727	15.663	39.022
							0.282436 ± 4	−11.88			
ASV5a			Aeolian Islands	0.704257[b]	0.512696[b]	1.13	0.282916 ± 11	5.10	19.528[b]	15.656[b]	39.314[b]
ALC11			Aeolian Islands	0.70371[c]	0.512864[c]	4.41	0.283096 ± 10	11.45	19.52[c]	15.64[c]	39.20[c]
FIL76			Aeolian Islands	0.70445[c]	0.512725[c]	1.70	0.283074 ± 6	10.69	19.50[c]	15.65[c]	39.23[c]
IBQ 1			Iblean Basin	0.70307[d]	0.51293[d]	5.70	0.282997 ± 11	7.96	19.812	15.652	39.456
IBQ 20			Iblean Basin	0.70285[d]	0.51306[d]	8.23	0.283020 ± 5	8.78	19.781	15.625	39.256
ET 75			Etna	0.703695[e]	0.51288[e]	4.72	0.283019 ± 6	8.74	19.873	15.679	39.603
CSE 12/5/97			Etna				0.282963 ± 4	6.75	19.908	15.672	39.621
VS9654t			Vesuvius	0.707191 ± 8	0.512468 ± 12	−3.32	0.282784 ± 6	0.44	19.069	15.631	39.134
VS9649t			Vesuvius	0.707179 ± 11	0.512485 ± 12	−2.98	0.282786 ± 6	0.48	18.935	15.529	38.862
651-44-2			Tyrrhenian Sea	0.70576[f]			0.282971 ± 8	7.02			
651-49-1			Tyrrhenian Sea	0.70438[f]	0.51294[f]	5.89	0.283075 ± 13	10.71	18.834	15.644	38.967
651-53-2			Tyrrhenian Sea	0.70733[f]			0.282973 ± 6	7.10	18.919	15.677	39.183
655-1-4			Tyrrhenian Sea	0.70384[f]			0.283207 ± 4	15.38			
655-2-2			Tyrrhenian Sea	0.70393[f]			0.283182 ± 7	14.50			
655-3-3			Tyrrhenian Sea	0.70372[f]			0.283174 ± 8	14.22			
655-5-1			Tyrrhenian Sea	0.70451[f]			0.283114 ± 5	12.09			
655-6-1			Tyrrhenian Sea	0.70434[f]			0.283129 ± 7	12.61			
655-10-3			Tyrrhenian Sea	0.70375[f]	0.51309[f]	8.82	0.283197 ± 5	15.03	18.714	15.581	38.700
655-12-1			Tyrrhenian Sea	0.70375[f]	0.51311[f]	9.21	0.283170 ± 6	14.09	18.698	15.573	38.666

[a]Sr and Nd isotope compositions were measured on a multicollector Finnigan MAT 262 mass spectrometer in Pisa following the elemental separation procedure of *Clocchiatti et al.* [1994]. Hf and Pb isotope compositions were determined by multicollector magnetic sector inductively coupled plasma-mass spectrometry using the VG model Plasma 54 in Lyon. Hf chemical purification followed the method outlined by *Blichert-Toft et al.* [1997], while Pb chemical purification was done according to a slightly modified procedure of *Manhes et al.* [1978]. Uncertainties reported on Sr, Nd, and Hf measured isotope ratios are $2\sigma/n^{1/2}$ analytical errors in the last decimal place, where n is the number of measured isotope ratios. $^{87}Sr/^{86}Sr$ of the NBS-987 Sr-standard = 0.710226 ± 12 (n = 11); $^{143}Nd/^{144}Nd$ of the La Jolla Nd standard = 0.511855 ± 5 (n = 12); $^{176}Hf/^{177}Hf$ of the JMC-475 Hf standard = 0.28216 ± 1 (Hf standard run every third sample). $^{87}Sr/^{86}Sr$, $^{143}Nd/^{144}Nd$, and $^{176}Hf/^{177}Hf$ were normalized for mass fractionation relative to $^{86}Sr/^{88}Sr$ = 0.1194, $^{146}Nd/^{144}Nd$ = 0.7219, and $^{179}Hf/^{177}Hf$ = 0.7325, respectively. For Pb isotope analysis, samples were bracketed between NIST 981 standard splits and calculated with respect to the value reported for this standard by *Todt et al.* [1996]. The capability of MC-ICP-MS to reproduce TIMS Pb isotope measurements with a better precision is documented by *White et al.* [2000], and the more general aspects of the technique (mass fractionation, standard-sample bracketing, precision, accuracy) are discussed by *Maréchal et al.* [1999]. ε_{Nd} and ε_{Hf} values were calculated using $(^{143}Nd/^{144}Nd)_{CHUR(0)}$ = 0.512638 and $(^{176}Hf/^{177}Hf)_{CHUR(0)}$ = 0.282772, respectively.

[b]*Del Moro et al.* [1998].

[c]*Francalanci et al.* [1993].

[d]*Tonarini et al.* [1996].

[e]*Clocchiatti et al.* [1994].

[f]*Beccaluva et al.* [1990].

[8] The volcanics from the RMP and TMP have relatively homogeneous Pb isotope compositions (Figure 5) and partially overlap the Pb isotope field of the Campanian region [*Hawkesworth and Vollmer*, 1979]. The Pb isotope compositions plot above the northern hemisphere reference line (NHRL), within the field of pelagic sediments [*Ben Othman et al.*, 1989]. They also plot within the field of recent circum-Mediterranean granites [*Juteau et al.*, 1986]

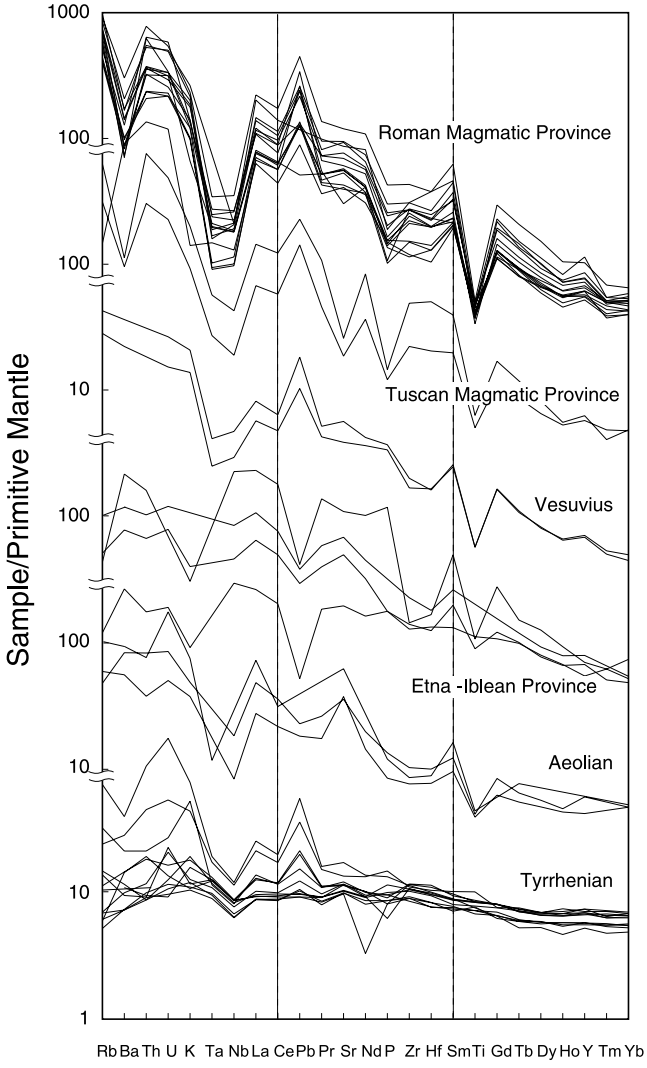

Figure 2. Primitive mantle-normalized [*Hofmann*, 1988] element variation diagrams for the Roman and Tuscan Magmatic Provinces (this work; Table A1), the Campanian Region [*Beccaluva et al.*, 1991], the Aeolian Islands [*Ellam et al.*, 1989], the Tyrrhenian Basin (this work; Table A1), and the Etna and Iblean Basin [*Armienti et al.*, 1989; *Beccaluva et al.*, 1998; *D'Orazio et al.*, 1997].

next to modern continental lead [*Stacey and Kramers*, 1975].

3.2. Southern Italy: Vesuvius, Aeolian Islands, Iblean Basin, Etna

[9] The magmas from the Campanian region (Vesuvius, Roccamonfina) and Aeolian Islands represent the transition between the RMP–TMP group and Etna. Although they have similar subduction-related geochemical characteristics, they are less enriched and display trace element anomalies that are less pronounced than magmas from the RMP and TMP (Figure 2). Markedly different geochemical patterns are observed for the Etna–Iblean basalts, which, at least until their very recent replacement by subduction-type compositions, are characterized by a plume-type signature (Figure 2) with conspicuous lack of Nb and Ta depletion [see also *Schiano et al.*, 2001].

[10] The isotopic compositions of the samples from southern Italy are plotted in Figures 3, 4, and 5, along with additional samples from the literature. The data show a progressive southward decrease of $^{87}Sr/^{86}Sr$ and an increase of ε_{Nd} and ε_{Hf} from Vesuvius to Etna and the Iblean Basin. In ε_{Hf}–ε_{Nd} space (Figure 4), the Vesuvius volcanics, just like the RMP and TMP volcanics, plot above the mantle–crust array within the field of pelagic sediments. By contrast, the Etna and Iblean Basin samples fall well below the regression line for the mantle–crust array [*Vervoort et al.*, 1999], in the field of HIMU basalts (not shown). Two of the Aeolian basalts plot within the mantle array and one plots slightly above it. The Pb isotope compositions show a range of $^{206}Pb/^{204}Pb$ and, to a lesser extent, $^{208}Pb/^{204}Pb$, consistent with the variations observed for the other isotopic systems (Figure 5). By contrast, $^{207}Pb/^{204}Pb$ remains rather constant. In Pb isotope space, the Etna and Iblean Basin samples fall within the field of northern-hemisphere oceanic basalts.

3.3. Tyrrhenian Sea

[11] The Tyrrhenian Sea samples from Site 655 (Leg 107) show mid-ocean-ridge basalt (MORB)-like geochemical patterns, but with a small negative Nb anomaly and a positive Pb anomaly (Figure 2). Samples from Site 651 show stronger enrichment in the most incompatible elements, with spikes at U and Pb and troughs at Ta and Nb (Figure 2), all in good agreement with their calc-alkaline character [*Beccaluva et al.*, 1990]. The Sr, Nd [*Beccaluva et al.*, 1990], and Hf isotope compositions all fall at the enriched end of the MORB array (Figures 3 and 4). The Pb isotope compositions, which are substantially more radiogenic than typical for normal MORB, are consistent with those obtained by *Hamelin et al.* [1979] on samples from the DSDP leg 42A (Figure 5).

4. Discussion

4.1. Mixing Relationships

[12] The isotopic compositions of the samples from the Tyrrhenian Sea are tightly grouped and, in agreement with previous findings [*Hamelin et al.*, 1979], are distinct from the rest of the Italian volcanics. These samples show a strongly depleted mantle signature, probably somewhat modified by the incorporation of sedimentary and other subduction-related material [*Beccaluva et al.*, 1990].

[13] In contrast, samples from the TMP, RMP, Vesuvius, Aeolian Islands, and the Etna–Iblean Basin define smooth mixing hyperbolas in $^{87}Sr/^{86}Sr$–$^{206}Pb/^{204}Pb$–ε_{Nd}–ε_{Hf} space (Figure 6; Hf not shown). *Vollmer* [1976] and later others [*Ellam et al.*, 1989; *Rogers et al.*, 1985] previously identified hyperbolic relationships in $^{206}Pb/^{204}Pb$–$^{87}Sr/^{86}Sr$ space that they interpreted quantitatively as a binary mixture. The hyperbolic arrays are well defined and the range of compositions among the TMP, RMP, Vesuvius, Aeolian Islands, and Etna–Iblean mafic lavas can be considered as remarkably restricted. Strongly curved mixing hyperbolas are particularly valuable because the position of the asymptotes narrowly constrain the position of the end-members [*Juteau et al.*, 1986]. We used the regression techniques decribed by

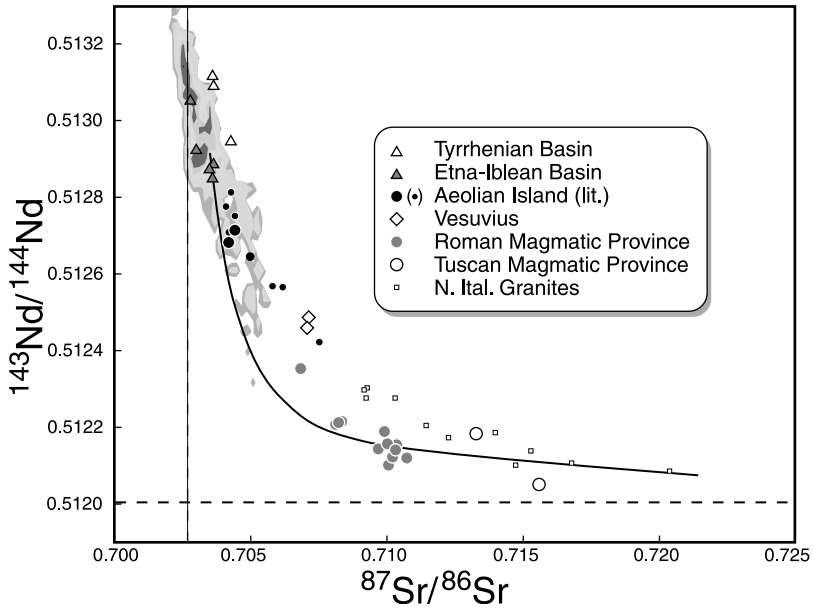

Figure 3. Plot of $^{143}Nd/^{144}Nd$ versus $^{87}Sr/^{86}Sr$ for Italian volcanics. Literature data sources are: Aeolian Islands (Alicudi, Filicudi, and La Sommata): *Del Moro et al.* [1998]; Aeolian Islands (Stromboli, Salina and Vulcano): *Ellam et al.* [1989]; Etna: *D'Orazio* [1994] and S. Tonarini (unpublished data, 1999); Iblean Basin: *Tonarini et al.* [1996]; Tyrrhenian Basin: *Beccaluva et al.* [1990]; N. Ital. granites: *Juteau et al.* [1986]. The mixing hyperbola was done by least squares regression (see text). The mantle array is displayed as a density diagram (grey shading) contoured at 95, 90, 66, 50 and 33% from numerous literature data (courtesy A.W. Hofmann).

Albarède [1995] to fit the data of the four binary diagrams that show the strongest curvatures: ε_{Nd} versus $^{87}Sr/^{86}Sr$, ε_{Hf} versus $^{87}Sr/^{86}Sr$, ε_{Nd} versus $^{206}Pb/^{204}Pb$, and $^{87}Sr/^{86}Sr$ versus $^{206}Pb/^{204}Pb$. The output parameters are the abscissa of one asymptote, the ordinate of the other asymptote, and a parameter c that describes the curvature of the hyperbola (Table 2; Figures 3 and 6). Error propagation was estimated through a set of 200 Monte Carlo simulations using the

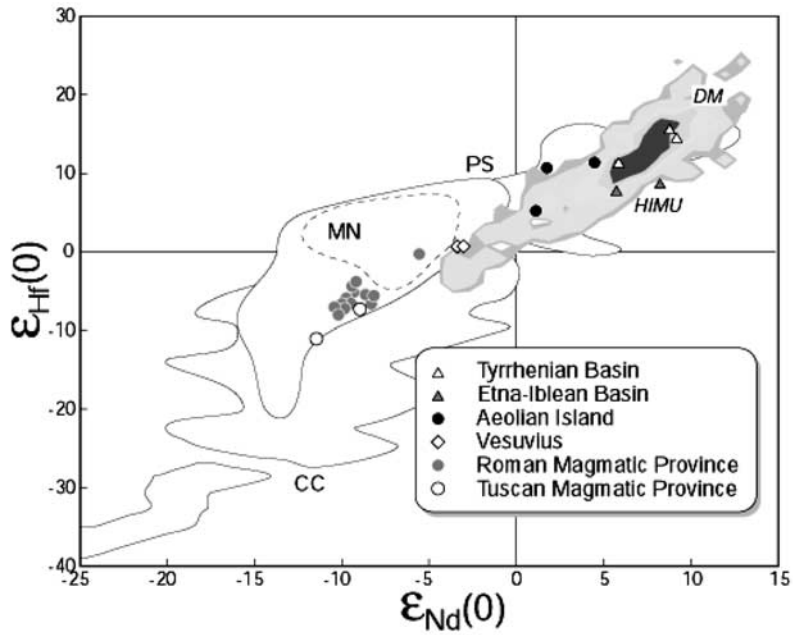

Figure 4. Plot of ε_{Hf} versus ε_{Nd} for Italian volcanics. Sources of Nd isotope data as in Figure 3. The mantle array is displayed as a density diagram (grey shading) contoured from more than 1000 published and unpublished data (courtesy J. Blichert-Toft). The crustal array is from *Vervoort et al.* [1999, 2000], the Mn-nodule field (MN) from *Albarède et al.* [1998], and the pelagic sediment field (PS) from *Vervoort et al.* [1999].

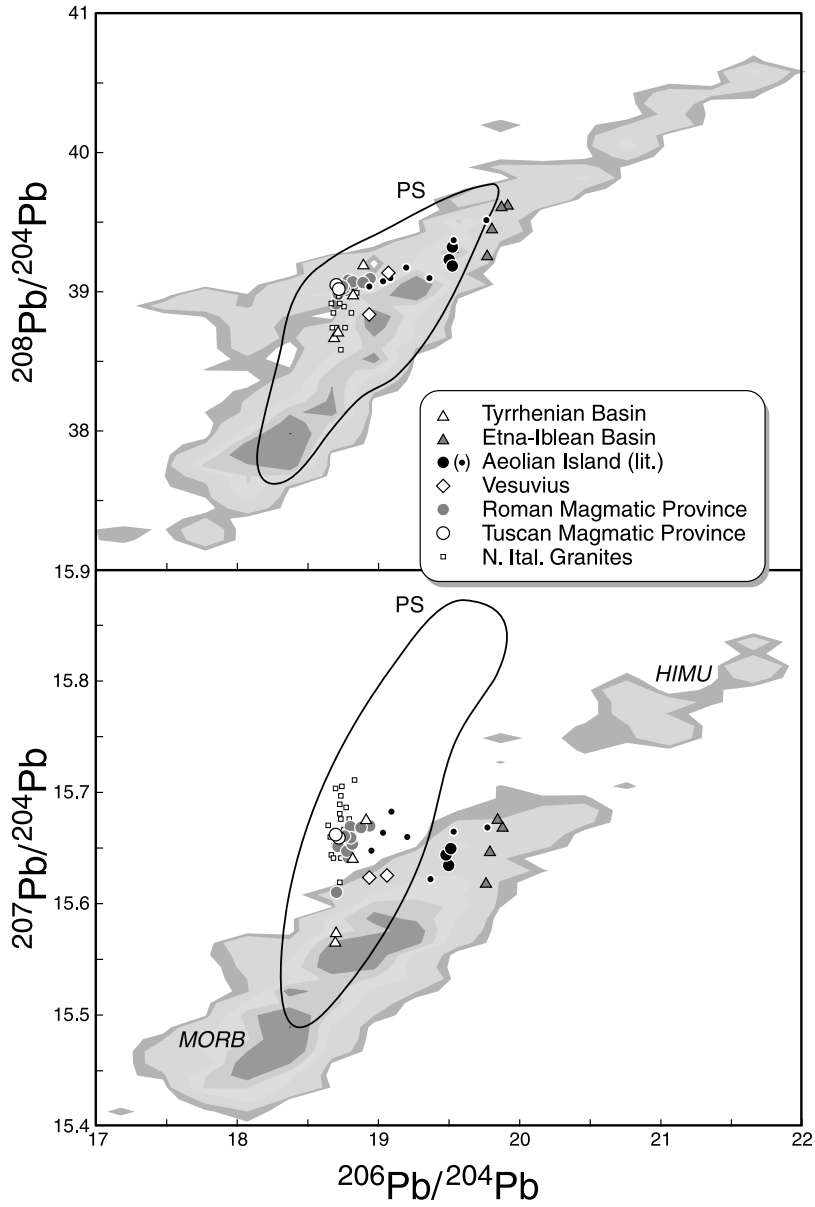

Figure 5. Plot of $^{208}Pb/^{204}Pb$ versus $^{206}Pb/^{204}Pb$ (top panel) and $^{207}Pb/^{204}Pb$ versus $^{206}Pb/^{204}Pb$ (bottom panel) for Italian volcanics. Sources of Pb isotope data are: Aeolian Islands: *Del Moro et al.* [1998] and *Francalanci et al.* [1993]; N. Ital. Granites: *Juteau et al.* [1986]; Tyrrhenian Basin (DSDP, Leg 42A): *Hamelin et al.* [1979]. Pelagic sediments (PS): numerous references (courtesy B.B. Hanan). The mantle array is displayed as a density diagram (grey shading) contoured from hundreds of data points from the PETDB database for MORB (http://petdb.ldeo.columbia.edu/petdb) and the GEOROC database for OIB (http://georoc.mpch-mainz.gwdg.de) and courtesy of A.W. Hofmann.

reproducibility of our in-house standards as input parameters. The bottom panel of Table 2 lists our best estimates of the compositions of the two end-members. Whenever the same isotopic composition of an end-member could be estimated from two separate binary plots, the results were consistent. These results unambiguously identify two distinct components: one with mantle characteristics and one with continental crust characteristics. The $^{206}Pb/^{204}Pb$ ratio of the mantle-derived (19.8) and crust-derived (18.5) components, as well as the $^{87}Sr/^{86}Sr$ ratio of the mantle component (0.7025–7028), are particularly well defined. Some of the other isotopic ratios of the end-member components, notably $^{87}Sr/^{86}Sr$ in the crustal component, cannot be as well constrained because of unfavorable curvature relationships. *Rogers et al.* [1985] and *Ellam et al.* [1989] further advocated the presence of a third component. Although it may be correct that the crustal component represents a range of Sr and Nd isotope compositions, this is not substantiated by Pb isotopes. Most Pb isotopic data from the literature spread along the $^{207}Pb/^{204}Pb$ axis, but that may simply reflect analytical difficulties associated with mass fractionation correction of this isotope ratio when measured by TIMS.

[14] Unfortunately, it is impractical to exploit these hyperbolic relationships further by calculating elemental ratios

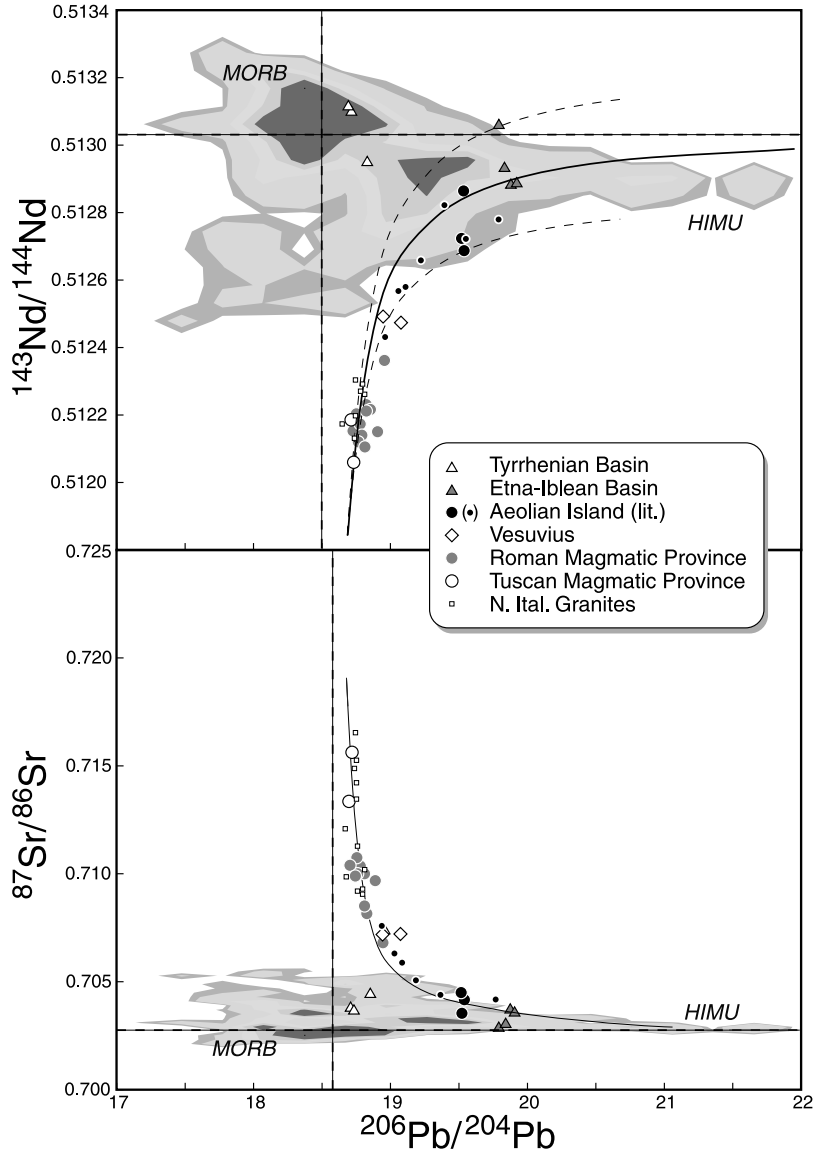

Figure 6. Plot of $^{143}Nd/^{144}Nd$ versus $^{206}Pb/^{204}Pb$ (top panel) and $^{87}Sr/^{86}Sr$ versus $^{206}Pb/^{204}Pb$ (bottom panel) for Italian volcanics. Sources of Nd and Sr isotope data as in Figure 3 and of Pb isotope data as in Figure 5. Mixing hyperbolas were calculated by least squares regression (see text). The mantle array is shown as a density diagram similar to those Figures 3, 4, and 5.

from the curvatures. We illustrate this point with the $^{143}Nd/^{144}Nd$ versus $^{87}Sr/^{86}Sr$ diagram and two end-members labeled M (mantle component) and C (crustal component), that plot at an unknown position along the mixing hyperbola (Figure 3). Using the expressions developed by *Albarède* [1995, p. 19], we obtain:

$$\frac{(S_r/Nd)_C}{(S_r/Nd)_M} = \frac{(^{87}Sr/^{86}Sr)_M - (^{87}Sr/^{86}Sr)_\infty}{(^{87}Sr/^{86}Sr)_C - (^{87}Sr/^{86}Sr)_\infty} = \frac{(^{143}Nd/^{144}Nd)_C - (^{143}Nd/^{144}Nd)_\infty}{(^{143}Nd/^{144}Nd)_M - (^{143}Nd/^{144}Nd)_\infty}$$

where the ∞ subscript refers to the asymptote position. One of the two differences in each ratio involving isotopic data is necessarily known with a poor relative precision: in this particular case, the asymptote intercept is very close to the mantle value on the Sr axis and to the crustal value on the Nd axis. Only relative values of the Sr/Nd ratio in each end-member can therefore be retrieved. Based on the elemental ratios determined in this way from the parameters of the different hyperbolas, the order of enrichment into the crust with respect to the mantle is Pb > (Nd, Hf) > Sr. This somewhat unexpected order, because Sr is commonly perceived as slightly more incompatible than both Nd and Hf [e.g., *Hofmann*, 1988], may hint at some unknown complexities of the crust-forming processes.

[15] No attempt was made to use mixing relationships that involve trace element concentrations. Even incompatible element ratios may be modified upon melting, while fractional crystallization may change the concentrations of these elements to a large extent. In addition, "mixing"

Table 2. Least Squares Mixing Hyperbolas for Volcanic Rocks From Central and Southern Italy[a]

Parameters of the Least Squares Mixing Hyperbolas			
	Asymptotes		Curvature
Correlation	x_∞	y_∞	c
$^{206}Pb/^{204}Pb - {}^{87}Sr/^{86}Sr$	18.61 ± 2	0.70254 ± 15	0.00125 ± 16
$^{206}Pb/^{204}Pb - {}^{143}Nd/^{144}Nd$	18.497 ± 7	0.51304 ± 6	−0.00023 ± 57
$^{87}Sr/^{86}Sr - {}^{143}Nd/^{144}Nd$	0.7028 ± 5	0.51204 ± 6	(9.217 ± 4) 10^{-7}
$^{87}Sr/^{86}Sr - {}^{176}Hf/^{177}Hf$	0.7025 ± 8	0.28246 ± 5	(8.97 ± 1) 10^{-7}

Estimated Isotopic Compositions of the Mantle and Crust End-members					
	Correlation	$^{87}Sr/^{86}Sr$	ε_{Nd}	$^{206}Pb/^{204}Pb$	ε_{Hf}
Mantle	Sr–Pb	∼0.7025 ± 1	–	∼19.8[b]	–
	Nd–Pb	–	∼8 ± 2	∼19.8[b]	–
	Nd–Sr	∼0.7028 ± 5	–	–	–
	Hf–Sr	∼0.7025 ± 7	–	–	∼8.7[b]
Crust	Sr–Pb	∼0.715[b]	–	∼18.61 ± 2	–
	Nd–Pb	–	–	∼18.50 ± 1	–
	Nd–Sr	∼0.715[b]	∼−12 ± 2	–	–
	Hf–Sr	∼0.715[b]	–	–	∼−11 ± 2

[a]Top: Positions of the asymptotes on the axes and constants of curvatures of least-squares mixing hyperbolas for isotopic data on Plio-Pleistocene and Quaternary Italian volcanics (see Figures 3 and 6). Bottom: Estimate of the isotopic compositions of the mantle and crust end-members.
[b]Extrapolated from several correlations.

diagrams such as $^{87}Sr/^{86}Sr$ versus 1/[Sr] used extensively in the literature, have been shown not to be diagnostic of mixing relationships, since linear relationships in this and other similar types of plots are accounted for just as well by the combined processes of assimilation and fractional crystallization (AFC) [*Albarède*, 1995; *Fleck and Criss*, 1985].

4.2. Nature of the Crust-Derived Component

[16] The presence of a crust-derived component in the Italian basaltic lavas was inferred early on from a variety of arguments, but most notably on the basis of ubiquitously high values of $\delta^{18}O$ [*Turi and Taylor*, 1976]. The $^{206}Pb/^{204}Pb$ ratio of the crustal end-member (18.5) is very similar to that of common lead [*Stacey and Kramers*, 1975], as well as to that of young granites from Tuscany and elsewhere around the Mediterranean region [*Juteau et al.*, 1986]. Although the ε_{Nd}, ε_{Hf}, and $^{87}Sr/^{86}Sr$ ratios (> 0.715) of this crustal component could fit a variety of local upper crustal sediments or magmas [*Ferrara et al.*, 1989; *Hawkesworth and Vollmer*, 1979], material other than that present in the Italian crust may have contributed to the composition of the crustal component. It is now widely accepted that this crustal component was not incorporated upon shallow-level interaction of pristine magmas with continental crust, but rather that it was present at depth within the mantle source or its surroundings [*Ellam et al.*, 1989; *Hawkesworth and Vollmer*, 1979].

[17] The potassic character of some of the Italian volcanics is closely related to the origin of the crustal component. Figure 7 (top panel) shows a steep increase of both Ce/TiO_2 and K_2O/TiO_2 ratios toward crustal values that cannot simply be due to fractional crystallization. At least 60% fractional crystallization would be required to account for this extent of variation, which is not consistent with the high Mg# and otherwise primitive character of these volcanics [*Civetta et al.*, 1989; *Peccerillo*, 1999]. Plotting Ce/TiO_2 versus K_2O/TiO_2 (Figure 7, top panel), where incompatible trace element abundances are normalized to TiO_2, the oxide of an incompatible element, in order to avoid the effect of phenocrysts and olivine ± clinopyroxene fractionation, demonstrates that the K enrichment is a spectacular effect of the otherwise general LILE enrichment during melting that characterizes the RMP and TMP volcanics. Enrichment in other very incompatible elements, such as U, Th, and La may be even more pronounced than that of K: the mean K/U ratio of the TMP and RMP lavas is on the order of 6000, i.e., nearly a factor of two lower than the accepted planetary value [*Jochum et al.*, 1983] and lower even than crustal averages [*Rudnick and Fountain*, 1995; *Taylor and McLennan*, 1995]. With the notable exception of Ti, Nb, and Ta, this enrichment follows the order of incompatibility accepted for magmatic processes [*Hofmann*, 1988] and does not seem to require the presence of a particular metasomatic agent, e.g., water or carbon dioxide. Plotting $^{206}Pb/^{204}Pb$ versus K_2O/TiO_2 (Figure 7, bottom panel) leads to two conclusions: (1) the K excess is mostly carried by the crustal component and not the mantle component (in agreement with, e.g., *Rogers et al.* [1985]) and (2) the range of K_2O/TiO_2 observed for the low $^{206}Pb/^{204}Pb$ crustal end-member together with the lack of hyperbolic mixing relationships for the RMP and TMP lavas require that the K_2O/TiO_2 ratio is strongly fractionated upon melting when enough crustal component is present in the source. The enrichment of Italian high-K volcanics in very incompatible elements therefore reflects the incorporation of low-degree melts of a source rich in continental detritus into dilute, large-degree basaltic melts, a point that will be returned to below. Whether this process should be categorized as metasomatic in nature is probably no longer a relevant issue.

[18] To understand the geodynamics associated with the Italian volcanics, one critical question is whether the crustal component is of pelagic or terrigenous origin. A pelagic component can either be associated directly with the subduction process, as argued for the Italian volcanics by *Rogers et al.* [1985] and *D'Antonio et al.* [1996], or may be an ancient recycled component of the mantle source itself, such as inferred for Hawaiian lavas [*Blichert-Toft et al.*, 1999a]. Although pelagic sediments trapped in the Italian crust

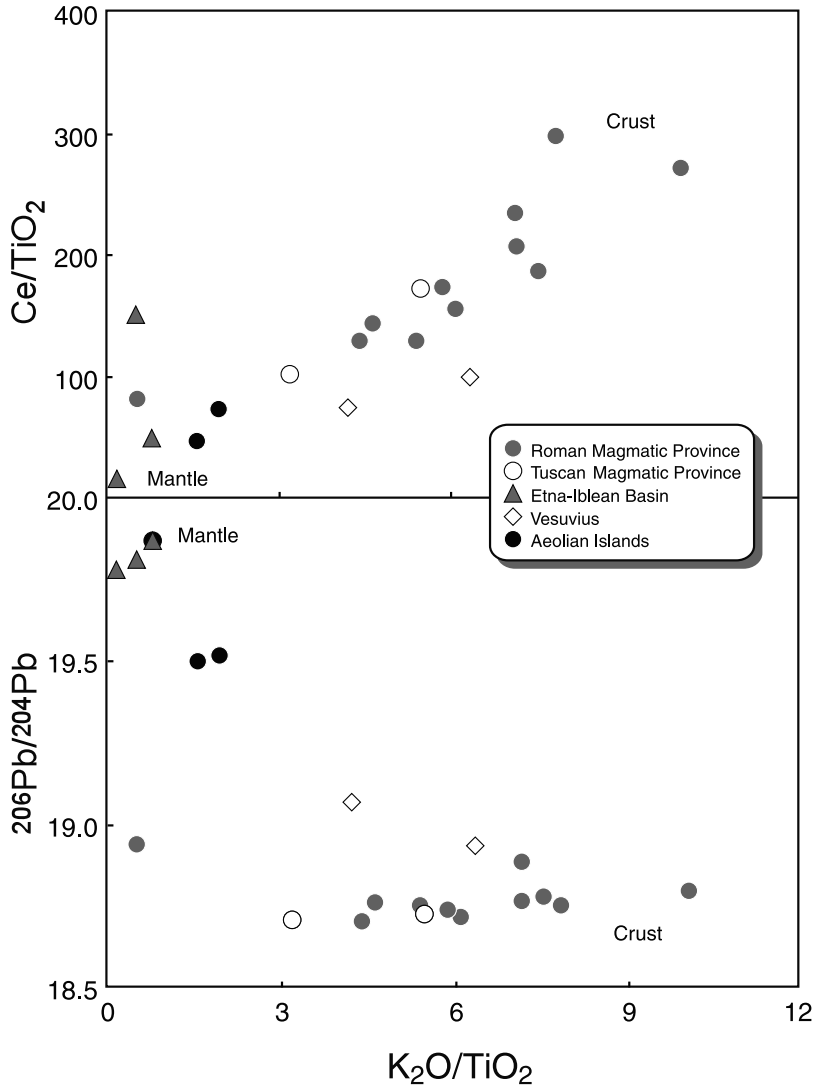

Figure 7. Plot of Ce/TiO_2 versus K_2O/TiO_2 (top panel) and $^{206}Pb/^{204}Pb$ versus K_2O/TiO_2 (bottom panel) for Italian volcanics. Sources of data for Aeolian Islands, Etna, and Iblean Basin as in Figure 3. Vesuvius data are from A. Sbrana (personal communication, 1999).

during the Apennine collision could also be considered a possible candidate, they would not have the ubiquitous presence required by the smooth isotopic mixing relationships. A terrigenous component likewise could be a mantle component, such as the EMII component of the Societies hot spot [*White and Hofmann*, 1982]. Alternatively, such a component could originate from interaction of basaltic magmas with the accretionary prism or simply with upper layers of the Italian crust.

[19] Two parameters in the form of a trace element ratio (Sm/Hf) and two isotope ratios combined (ε_{Hf} and ε_{Nd}) can be used to evaluate the presence or absence of a pelagic component. Dense detrital zircons are concentrated on continental margins in detrital sediments and turbidites, whereas light argillaceous material can be transported over very long distances by oceanic currents and winds. Because Hf geochemically is very similar to Zr and is concentrated by up to several percent in refractory zircons, the net result is that pelagic material has a much lower relative abundance of Hf with respect to elements that are less concentrated in zircons than do turbidites and other clastic sediments [*Patchett et al.*, 1984; *Plank and Langmuir*, 1998; *Vervoort et al.*, 1999]. In Figure 8, the Sm/Hf ratio [*White and Duncan*, 1996], which is sensitive to this process, is plotted (as Hf/Sm) against $^{147}Sm/^{144}Nd$, the latter chosen in order to view the data as a function of a well-understood parameter depicting trends of depletion and enrichment by melting. The Hf/Sm ratio is particularly well suited to estimate the abundance of zircon in a crustal component and therefore the nature of its sedimentary protolith. In the vast majority of MORB and OIB, the Hf/Sm ratio is remarkably constant and very close to the chondritic value of 0.70 [*Blichert-Toft et al.*, 1999b; *Chauvel and Blichert-Toft*, 2001], demonstrating that it is not fractionated by melt generation in the mantle. In contrast, sediments in particular and continental crust in general display a large variability of this ratio that can be ascribed to zircon sorting. The average sediment arriving at subduction zones (GLOSS [*Plank and Langmuir*, 1998]) has a Hf/Sm ratio of 0.16, which indicates that oceanic sediments, as a general rule, are zircon-starved. At the other end of the scale, the average

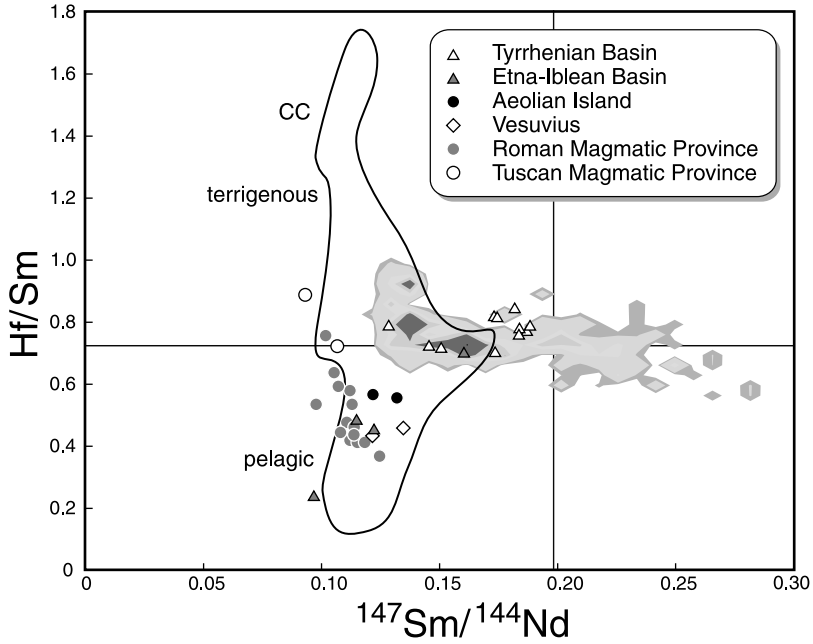

Figure 8. Plot of Hf/Sm versus $^{147}Sm/^{144}Nd$ for Italian volcanics. Data for MORB and OIB of the mantle array (shown as a density diagram in grey shading) and for pelagic and terrigenous sediments are from numerous references. Hf/Sm = 0.7 for chondrites.

continental crust is believed to have higher-than-chondritic Hf/Sm (0.85–0.95) [*Rudnick and Fountain*, 1995; *Taylor and McLennan*, 1995]. A low Hf/Sm ratio in basalts, such as is observed for many of the Italian volcanics in Figure 8, is therefore an unambiguous signal that pelagic sediments are present in their mantle source.

[20] The presence of a pelagic component in the source of the Roman and Tuscan basalts is also supported by their Hf–Nd isotope relationship. Following the original suggestion by *Patchett et al.* [1984], it was demonstrated that for a given ε_{Nd} value, ε_{Hf} of manganese nodules [*Albarède et al.*, 1998], which are proxies for pelagic sediment, and of pelagic sediments themselves [*Vervoort et al.*, 1999], plot well above the mantle–crust array. All the samples from the RMP and TMP plot in the upper part of or above the ε_{Hf}–ε_{Nd} mantle–crust array (Figure 4) as defined by a regression line with the equation of $\varepsilon_{Hf} = 1.33\ \varepsilon_{Nd} + 3.19$ (not shown) [*Vervoort et al.*, 1999]. This is particularly clear for the RMP basalts, which plot up to 5 epsilon units above *Vervoort et al.*'s [1999] OIB–MORB reference line and have Hf/Sm ratios (down to 0.3) lower than the chondritic value. This is also the case for some Aeolian lavas. For Etna and the Iblean Basin, the strong effect of the HIMU component (see below), which is located below the mantle array, somewhat counteracts the effect of pelagic sediments in ε_{Hf}–ε_{Nd} space (Figure 4), but these lavas still have Hf/Sm ratios as low as 0.23. Although the presence of a terrigenous component and shallow-level interaction of the magmas with local crust cannot be ruled out by the present data, especially for the RMP lavas, the predominant crustal effects on isotopes and trace elements seem to be those originating from a pelagic component.

4.3. Nature of the Mantle-Derived Component

[21] The mantle-derived component could be categorized simply as generic OIB, but we instead embrace the view that the chemistry of any basalt can be accounted for by components that can be traced back to lithological types formed in well-defined geodynamic environments. The nature of these components has been discussed often enough in the literature that we need not repeat this discussion here.

[22] It is unlikely that the mantle-derived component could be pure intermediate FOZO [*Hart et al.*, 1992] or C [*Hanan and Graham*, 1996]. First, the reality of these components (except for He that rarely correlates with other refractory isotopes) depends on the interpretation of crossing linear isotopic arrays at intermediate values: such an intersection may represent the common point of mixing trends at a mean value that does not necessarily have a specific lithological meaning. Second, it is possible to build the entire known isotopic reference frame without such an intermediate component. We therefore constructed our description of the mantle-derived component for the Italian volcanics such that it refers to well-known and well-defined isotopic end-members.

[23] Three different kinds of mantle-derived components dominate the most primitive Italian volcanics: DM (Depleted Mantle) in the Vavilov Basin (Tyrrhenian Sea) [*Beccaluva et al.*, 1990; this study], EMI (Type I Enriched Mantle) in Sardinia [*Gasperini et al.*, 2000], and HIMU (high-μ)-like mantle in the Etna–Iblean Basin [*Beccaluva et al.*, 1998; this study]. The isotopically extreme samples from Etna and the Iblean Basin do not correspond to a pure HIMU component, such as defined by samples from the HIMU type-localities of St Helena [*Sun*, 1980; *White and Hofmann*, 1982], Tubuai, and the Austral-Cook Islands [*Chauvel et al.*, 1992; *Vidal et al.*, 1984] (Figure 6). As previously pointed out by *D'Antonio et al.* [1996], they instead correspond to a mixture of HIMU and DM sources.

[24] The presence in volcanic series of binary mixtures that do not necessarily have pure end-members is relatively

common. Well-known examples are the Comores [*Class and Goldstein*, 1997; *Deniel*, 1998] and Hawaii [*Abouchami et al.*, 2000]. Isotopically homogeneous hot spots nevertheless seems to be able to tap a reproducible mixture of components for tens of millions of years (e.g., the Réunion hot spot [*Fisk et al.*, 1988; *Graham et al.*, 1990]). Mixtures of DM and HIMU in particular are prevalent in basalts from many ocean islands [*Chauvel et al.*, 1992; *Hofmann*, 1997] and from localities where mid-ocean ridges interact with plumes [*Schilling et al.*, 1992]. This does not necessarily require that the DM and HIMU components have been homogenized in the source, but rather that the length scale of heterogeneities is smaller than the characteristic length scale over which melt is extracted.

[25] The isotopic characteristics of the HIMU component reflect a mantle source with long-term evolution in a high-U/Pb and high-Th/Pb environment. Such an environment is commonly thought of as ancient altered oceanic crust stored in the mantle for long periods of time, typically 2 Ga or more [*Chase*, 1981; *Chauvel et al.*, 1992; *Hart et al.*, 1986; *Hofmann*, 1997; *Hofmann and White*, 1982]. Alternative models hold that the HIMU component is stored in the subcontinental lithosphere, where it originated through pervasive metasomatic interaction of strongly undersaturated melts, such as melilitite, with peridotite [e.g., *Hawkesworth et al.*, 1990]. In this model, it is possible to explain HIMU basalts in the oceanic environment through the remelting of subcontinental lithospheric mantle that has been delaminated and recirculated by mantle convection [*McKenzie and O'Nions*, 1983]. We prefer the interpretation calling for oceanic crust recycling over that involving metasomatized subcontinental lithospheric mantle. The formation and subduction of oceanic crust by plate tectonic processes represent processes on a large scale that have operated probably over most of Earth's history and generated well-understood magmatic products. By contrast, the nature and extent of metasomatic processes within the subcontinental lithosphere seem to be variable and small, thus calling into question their global importance for chemical inventories. From standard observations about MORB isotope geochemistry, we assume that the HIMU component is important in the deep mantle, but not in the asthenospheric upper mantle. This assumption does not imply that ancient oceanic crust is stored below any specific depth (e.g., 660 km), but rather that the abundance of ancient subducted material increases strongly with depth.

4.4. Contribution of the OIB Mantle to Italian Volcanism and Subduction History

[26] We will assume in the following that the HIMU component is typical of hot spot magmas. In order to use our present geochemical data to constrain the geodynamic regime beneath Italy and the relationship of this regime to the recent volcanism in the area, we must first understand how OIB melts can be present in a setting usually considered unfavorable to the emplacement of such magmas. As pointed out by *Morris and Hart* [1983] for the Aleutians, and as reiterated by *Ellam et al.* [1989] for the Italian volcanics, it is unlikely that a plume could burn through cold subducting lithosphere and produce volcanic chains parallel to the subduction boundary.

[27] We suggest that the timing and particular configuration of the subduction geometry of the Apennine collision explain why the Italian OIB-type basalts erupted in a subduction environment. During most of the Tertiary, the Adria plate was subducted westward under the European margin. This episode terminated at ca 13 Ma with the final stage of collision between the continental crusts of the two plates and the end of andesitic volcanism in Sardinia [*Argnani and Savelli*, 1999; *Beccaluva et al.*, 1985]. Deep earthquakes are conspicuously absent from central Italy, which *Westaway* [1992] considered as evidence against active shallow subduction in this area. The collision resulted in a rotation of the convergence and subduction azimuth toward the northwest with the opening of the Tyrrhenian Sea as a back arc basin at about 8 Ma [*Beccaluva et al.*, 1990]. Modern seismicity is ubiquitous under the southeastern Tyrrhenian Sea at depths of 200–500 km (Istituto Nazionale Geofisica, unpublished data, available at http://www.inrgm.it). The consequence of such a readjustment in the subduction direction is that the plate, which is now being subducted under Sicily, remains attached in the north to the part of the plate that was stalled or considerably slowed by the Apennine collision. The continuous distribution of earthquakes [*Meletti et al.*, 2000] and the continuity of the fast material (cold plate) at depths of 400–600 km below the Italian peninsula and Sicily (C. Piromallo and A. Morelli, P-wave tomography of the mantle under the Alpine-Mediterranean area, submitted to *Journal of Geophysical Research*, 2001) indicate the presence of a continuous subduction system at depth. However, there exists a substantial gradient in recent subduction velocities between the northern and southern parts of the subducting plate, on the order of a few cm/y, due to passive subduction (i.e., gravitational sinking) of ca 1 cm/y under Tuscany and active subduction of 5 cm/y under Sicily together with a sharp change in the subduction azimuth. Since the beginning of the opening of the Tyrrhenian Sea, therefore, the differential of subduction length between the two ends of the plate is about 300 km. Although trench roll-back and counterclockwise rotation of Italy may have absorbed some of this differential displacement between the north and the south, we surmise that this displacement is mostly accommodated by the rupture of the plate that would be torn off by such a large velocity gradient acting over such a short distance. A ca 400-km-wide NW–SE gap in the high-velocity material representing the subducting plate is observed under the southern part of the peninsula (e.g., under Vesuvius) at a depth of 150 km in the high-resolution tomographic model of C. Piromallo and A. Morelli (personal communication, 2000). Our proposition is further consistent with tomographic cross-sections showing low-velocity ("hot") material under Vesuvius down to depths in excess of 200 km [*Doglioni et al.*, 1999]. This contrasts with cross-sections under Tuscany and Sicily that reveal the presence of well-defined dipping slabs of high-velocity ("cold") material.

[28] Tomographic evidence therefore supports the existence of a broad window in the Adria plate under the southern part of the peninsula. The presence of an abundant HIMU component in basalts from southern Italy indicates that material from relatively deep mantle layers is channeled toward the surface and feeds major volcanoes such as

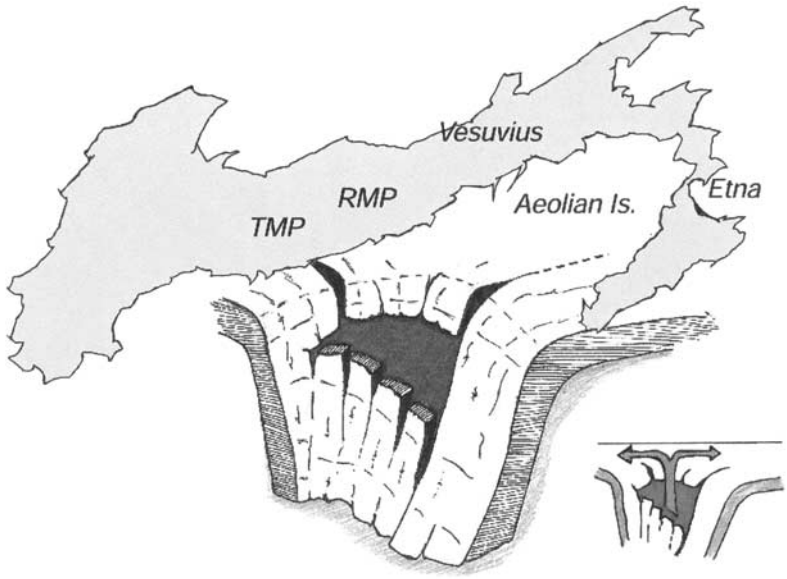

Figure 9. Cartoon showing the plate window in the Adria slab through which the counterflow of mixed upper and lower mantle is channeled to the upper part of the subducted slab.

Vesuvius. Such a channel may correspond to the continuous low-velocity region observed from the surface down to the transition zone beneath the southern part of the peninsula [*Doglioni et al.*, 1999].

[29] We further propose that the trailing upper edge of the plate section torn off below southern Italy induces a counterflow of mixed lower mantle and asthenosphere (Figure 9) that rises to replace the foundering material. This counterflow channeled into the plate window between the modern active subduction to the south and the fossil subduction to the north becomes the source of the mantle component in the Italian volcanics and accounts for the mixture of HIMU and DM components. This material may then spread laterally in the asthenospheric mantle wedge and be redistributed to the north and to the south where it becomes a more or less predominant component of essentially all Italian mafic volcanics. This model differs from the model of slab tear induced by gravitational pull of *Wortel and Spakman* [2000] by the active role played by the change in the direction of subduction. The narrow range of the isotopic properties of the mantle end-member over the entire magmatic province indicates that the vertical mixing between the HIMU and DM components in the counterflow is fairly efficient and steady. The nature of the flow regime that could make mixing efficient in such a relatively narrow channel is at present unknown. An alternative possibility that would alleviate the difficulties of a focused channel-flow is that a so-far undocumented hot spot is present beneath southern Italy and that its material is channeled through the plate window into the mantle wedge above the subduction zone.

[30] The northward increasing proportion of the crust-derived component in the mixture along the length of the volcanic province and the coincidence of its Pb isotope composition with that of modern sediments suggests that the pelagic material was incorporated at relatively shallow levels. This could have happened when rising mantle material interacted with the upper surface of the subducting slabs, either fossil as in the north or active as in the south. Another possibility is that melts interact with a depleted upper mantle modified by fluids extracted by dehydration of the subducting plate [*Hawkesworth and Vollmer*, 1979]. The distribution of end-members, however, favors thorough mixing between the HIMU and DM components and, therefore, vertical mixing across different mantle layers *prior to* incorporation of the crust-derived component. Moreover, if a substantial fraction of the mantle-derived material originated from the mantle wedge above the subduction zone, we would expect the Italian volcanics to be more calc-alkaline in character, similar to other orogenic series around the world. Such a signature is either weak [*Schiano et al.*, 2001] or absent.

[31] The gradient in the geochemical properties showing more crust-derived component in the north and more mantle-derived component in the south probably reflects both the relative strength of mantle material injection into the mantle wedge and the difference in thickness of the local crust. In the south, abundant mantle melts modified by interaction with the pelagic veneer of the plate are only slightly affected by the continental crust, which is either absent, as in the Tyrrhenian Basin or of limited extent. In Tuscany, smaller inputs of mantle melt from a more distant source are more efficiently modified by interaction with a thick and ubiquitous continental crust. This contrast is substantiated by the abundance of anatectic melts erupted contemporaneously with mafic rocks in the TMP [e.g., *Marinelli and Mittempergher*, 1966], whereas they are uncommon in the southern part of the Italian volcanic province.

4.5. Major Elements and Isotope Compositional Relationships: Assessing Mixing Ratios

[32] If mixing is conservative, the proportions of mantle material and melt involved in mixing processes can be retrieved from isotopic relationships [e.g., *Schilling et al.*, 1992]. The question remains, however, how major elements

correlate with isotopes. For example, basaltic rocks from the TMP carry a fully developed crustal isotopic signature impossible to obtain by mixing basalts and anatectic melts. Basaltic melts can only exhibit an isotopic signature characteristic of crustal material if the major element budget is largely decoupled from the trace element budget. Melting of a metasomatized mantle source or a source sprinkled with continental detritus (e.g., phlogopite peridotite, see references above) is inconsistent with the high K_2O/H_2O ratios (>3) of primary melt inclusions analyzed at Vulsini, (RMP [*Kamenetsky et al.*, 1995]). This ratio is on the ''dry'' side of the MORB range in contrast with subduction-zone primary magmas [*Sobolev and Chaussidon*, 1996]. Source enrichment in water with respect to other incompatible elements is undocumented, which suggests that melt production and transport, not fluid percolation, account for the overall geochemical compositions of the TMP and RMP basalts.

[33] Different melt migration configurations potentially may achieve such a decoupling, all based on the following principle: no melt is expected to preserve a nonbasaltic major element chemistry when it percolates through the mantle in which all major basalt-forming elements are largely available, regardless of the melting history of this mantle. The mantle matrix buffers, at least to some extent, the major element composition of the melt. Conversely, changes in the isotope geochemistry of the percolating melt critically depend on the availability of some particular trace elements in the ambient mantle, i.e., whether the mantle was depleted in Nd, Hf, Sr, Pb, etc. by previous melt extraction events. This reflects the property that major elements are moderately (Al, Na, Ti) to strongly (Mg, Si, Fe) compatible, whereas the trace elements that appear in common isotopic systems (except Os) behave as incompatible to highly incompatible elements. Fusion flushes trace elements from the residue but, unless the degree of melting is large, still leaves it relatively fertile with respect to major elements for further interaction with percolating melts. Such a contrasting behavior explains apparent inconsistencies such as how a basaltic rock can have a crustal isotopic signature but a basaltic major element chemistry, as in the case of the TMP. However, it unfortunately also makes the mixing ratios inferred from the isotope component inventories essentially irrelevant to the assessment of actual proportions of melt, mantle, and sediment involved in the mixing process.

5. Conclusions

[34] The curvature of the binary hyperbolic relationships defined by the Quaternary and Plio-Pleistocene Italian volcanics in $^{87}Sr/^{86}Sr-^{206}Pb/^{204}Pb-\varepsilon_{Nd}-\varepsilon_{Hf}$ space is sufficient to define the following end-members with good precision:

1. The mantle-derived end-member is a relatively homogeneous mixture of the standard HIMU and DM components.
2. The crust-derived end-member is responsible for the enrichment in K and other LIL elements. The relationship in $\varepsilon_{Hf}-\varepsilon_{Nd}$ space and the lower-than-chondritic Hf/Sm ratio indicate that this crustal component is dominated by pelagic and not terrigenous material.

[35] Plume-type magmas may be channeled from the lower mantle into the Italian volcanic provinces through a plate window formed by the differential of subduction velocity between the fossil plate beneath Tuscany and the active plate beneath Sicily. Vertical mixing of upper and lower mantle in the wake of the trailing edge of the rifted plate may produce the mantle source of Italian mafic volcanism. It is also possible that material from a so-far unidentified plume is channeled through the plate window. The crustal component is probably acquired by interaction of the mantle advected through the window with the upper part of the subducted plate. We further argue that mixing ratios inferred from the hyperbolic relationships cannot be used to constrain the actual proportions of mantle, melt, and sediment involved in the mixing process.

Appendix A: Geological Outline

A1. Northern Tyrrhenian Area: RMP and TMP

[36] The Plio-Pleistocene potassic magmatism of the internal sector of the northern Apennine chain took place in a postextensional tectonic setting. While some authors have interpreted this scenario as the result of anticlockwise rotation of the Apennine chain within a back arc extensional environment [*Argnani and Savelli*, 1999; *Bartole*, 1995; *Beccaluva et al.*, 1991; *Giunchi et al.*, 1996; *Meletti et al.*, 2000; *Serri*, 1997; *Tamburelli et al.*, 2000; *Wilson*, 1989], others believe that the magmatism of the RMP and TMP was related to lithospheric extension within an intraplate tectonic setting, such as the Eastern African Rift or the Rhine graben [*Lavecchia and Stoppa*, 1991; *Liotta et al.*, 1998].

[37] The time of onset of potassic magmatism in the RMP and TMP is a matter of debate: most authors consider the small lamproitic outcrop at Sisco, North Corsica (about 14 Ma [*Bellon*, 1981; *Civetta et al.*, 1978; *Serri et al.*, 1993]) to be the first magmatic event in this area. However, the large spatial and temporal gap between the isolated Corsican episode and the beginning of the oldest potassic magmatic activity in the Tuscan region some 10 My later (Orciatico and Montecatini Val di Cecina lamproites: 4.1 Ma [*Ferrara et al.*, 1989]) makes this interpretation controversial. Felsic intrusive and extrusive magmatism took place in southern Tuscany and in the Tuscan archipelago between 7 to 2.2 Ma [*Ferrara et al.*, 1988; *Lombardi et al.*, 1974; *Serri et al.*, 1993]. This was followed by migration of the magmatism from west to east, with the emplacement of, in turn, Radicofani (1.3 Ma [*Innocenti et al.*, 1992]), Cimini, and Torre Alfina volcanics (1.3–0.8 Ma [*Conticelli*, 1998; *Fornaseri*, 1985]) in the TMP and the Pleistocene potassic and ultrapotassic rocks in the RMP (Latium; 0.6 Ma to 0.08 Ma [*Barberi et al.*, 1991; *Cioni et al.*, 1993; *Laurenzi and Villa*, 1987]).

[38] The TMP is characterized by coexistence of both plutonic and volcanic rocks of subalkaline (acidic and high-K calc-alkaline) to potassic alkaline (intermediate and acidic) and ultrapotassic (lamproites, latites, and shoshonites) affinity [*Serri et al.*, 1993, and references therein]. By contrast, the rocks from the RMP are exclusively volcanic and comprise only potassic alkaline compositions, which have been divided into two geochemical groups on the basis of their K_2O/SiO_2 ratio [*Beccaluva et al.*, 1994; *Foley et al.*, 1987; *Marinelli*, 1975; *Peccerillo*, 1998; *Peccerillo et al.*, 1987; *Serri et al.*, 1993, 1991; *Wilson*, 1989]. The potassic series (KS) consists of saturated to oversaturated volcanic rocks ranging from trachybasalts to rhyolites, whereas the

Table A1. Major and Trace Element Concentrations for the Most Primitive Volcanic Rocks From the Roman and Tuscan Magmatic Provinces and for Samples From the Tyrrhenian Basin[a]

Sample	DG1	V849B	V972	V971	VS229	VS230	VS228	VS224	V975	V976	V977	DMS984	DMS983	DME981	DME982
Locality	A Vico RMP	N Vico RMP	N Vico RMP	N Vico RMP	L Vulsini RMP	L Vulsini RMP	M Vulsini RMP	M Vulsini RMP	M Vulsini RMP	M Vulsini RMP	M Vulsini RMP	MM Sabatini RMP	B Sabatini RMP	SS Ernici RMP	SG Ernici RMP
SiO_2	50.70	49.29	50.30	47.06	51.60	53.95	46.14	49.43	47.67	46.99	48.31	49.52	46.95	44.58	47.34
TiO_2	0.86	0.75	0.76	0.74	0.91	0.71	0.83	0.61	0.70	0.68	0.70	0.67	0.93	0.87	0.81
Al_2O_3	16.31	16.17	16.18	16.36	18.11	16.99	17.82	15.90	11.79	14.40	13.82	16.55	17.79	22.80	17.41
Fe_2O_3	8.26	3.90	3.10	7.36	7.14	0.70	3.80	1.38	5.18	1.83	4.43	2.64	3.93	4.48	3.37
FeO	0.00	3.98	4.62	1.25	0.94	4.90	4.67	4.92	2.95	5.45	3.39	4.33	5.40	3.85	4.20
MnO	0.13	0.15	0.14	0.15	0.14	0.11	0.15	0.13	0.15	0.14	0.14	0.13	0.17	0.15	0.15
MgO	4.37	7.20	7.20	7.41	4.14	7.44	5.69	10.28	13.12	10.40	9.46	6.73	3.84	8.24	6.50
CaO	8.25	11.32	10.25	12.89	8.48	7.40	11.54	10.17	13.11	13.58	14.25	10.03	10.35	8.42	10.62
Na_2O	1.75	1.78	3.06	1.50	1.92	2.58	1.89	1.76	1.22	1.46	1.46	1.43	1.51	1.70	2.15
K_2O	8.18	4.40	2.06	3.77	5.53	4.16	6.24	4.35	3.07	3.14	3.77	6.71	7.28	0.44	5.79
P_2O_5	0.39	0.29	0.32	0.30	0.42	0.22	0.50	0.34	0.21	0.32	0.28	0.62	0.88	0.31	0.53
L.O.I.	0.79	0.79	2.01	1.22	0.65	0.84	0.73	0.74	0.84	1.60	1.07	0.64	0.97	4.17	1.14
Total	99.99	100.02	100.00	100.01	99.98	100.00	100.00	100.01	100.01	99.99	101.08	100.00	100.00	100.01	100.01
mg#	54.31	66.03	66.27	65.55	53.19	73.12	58.71	77.13	77.70	74.76	72.17	66.99	46.49	67.88	64.50
V	218	250	232	205	257	168	302	195	207	212	227	272	326	267	263
Cr	51	249	243	256	29	356	20	792	1180	833	955	258	34	359	284
Co	30	34.0	32.4	33.5	28.4	99.5	37.4	35.9	42.6	39.2	33.5	33.1	34.7	40.1	31.7
Ni	45	66.9	60.6	74.8	20.9	192	40.2	205	277	198	228	76.3	15.3	58.1	66.4
Rb	457	344	381	309	376	312	402	273	215	226	236	524	488	7.84	392
Sr	1576	1047	1014	1024	1268	552	1395	1106	718	968	778	1728	2178	744	1692
Ba	1252	526	500	444	847	426	870	773	529	592	616	1013	1835	551	1039
Cs	n.d.	20.1	19.5	20.3	18.2	14.7	26.0	15.4	14	14.6	13.9	31.5	36.0	1.12	22.6
Y	45	22.0	22.5	24.3	28.4	26.7	33.7	25.6	20.5	21.7	24	30.2	40.5	24.1	30.7
Zr	301	205	216	234	268	263	262	248	146	148	111	299	419	116	263
Hf	n.d.	5.3	5.25	5.32	6.64	6.23	5.98	5.35	3.46	3.78	3.48	7.13	10.1	2.78	6.07
Nb	13	11.2	11.1	11.4	13.9	16.5	11.8	16.1	6.21	7.07	6.00	13.1	21.7	8.00	12.8
Ta	n.d.	0.70	0.69	0.74	0.84	0.96	0.59	0.87	0.33	0.36	0.32	0.66	1.21	0.52	0.56
La	124	48.0	46.7	49.6	67.6	66.2	71.3	74.2	41.3	47.9	43.3	90.1	136	38.9	85.0
Ce	223	102	101	104	142	123	155	143	90.6	97.9	90.8	182	277	70.5	168
Pr	24	12.5	12.5	12.7	17.6	13.3	17.7	16.2	10.3	11.3	10.8	23.0	33.0	8.8	19.7
Nd	96.9	50.6	49.1	48.5	67.2	48.9	70.4	62.2	43.6	44.4	42.6	88.2	129	36.6	77.9
Sm	17.8	8.91	9.02	8.38	12.4	8.2	12.7	10.0	7.76	8.3	7.95	17.2	24.2	7.48	14.4
Eu	3.38	1.92	1.96	1.81	2.56	1.59	2.67	2.23	1.88	1.84	1.63	3.27	4.96	1.76	2.97
Gd	11.8	6.49	6.54	6.62	8.2	5.86	9.57	7.38	6.26	6.59	5.66	11.2	15.2	5.73	9.97
Tb	1.43	0.88	0.85	0.87	1.07	0.85	1.24	0.98	0.77	0.84	0.76	1.28	1.95	0.75	1.37
Dy	7.18	4.52	4.25	4.39	5.45	4.74	5.9	5.00	3.78	4.02	4.27	6.48	9.71	4.18	6.37
Ho	1.18	0.79	0.80	0.79	0.97	0.88	1.06	0.87	0.65	0.7	0.77	1.02	1.49	0.81	1.03
Er	0.35	0.28	0.30	0.32	2.48	2.21	2.56	2.31	1.82	1.86	1.87	2.26	3.53	1.96	2.58
Tm	0.35	0.28	0.30	0.32	0.31	0.33	0.35	0.32	0.25	0.26	0.24	0.32	0.44	0.32	0.33
Yb	2.21	1.76	1.8	2.15	2.1	2.29	2.42	2.02	1.65	1.78	1.66	2.14	2.70	1.93	2.13
Lu	0.32	0.26	0.26	0.31	0.32	0.36	0.34	0.32	0.25	0.28	0.26	0.28	0.37	0.26	0.29
Pb	n.d.	21.8	22.4	8.95	23.0	41.7	38.1	59.6	22.3	45.8	23.7	45.0	78.4	15.6	42.1
U	10.2	5.19	6.43	6.77	5.94	6.89	6.79	11.9	4.40	4.67	4.42	9.98	11.0	2.41	6.37
Th	43.1	26.5	26.0	28.9	29.6	50.7	30.4	52.0	19.1	19.3	16.9	44.8	63.4	11.0	30.2

Table A1. (continued)

Sample	VS221	VS232	655-B-01(116)	655-B-02	655-B-03	655-B-05	655-B-06	655-B-010	655-B-010(49)	655-B-012	655-B-012(95)	651-A-044	651-A-049	651-A-053
Locality	C Radicofani TMP	CP Cimini TMP	GR VB TB	GR VB TB	GR VB TB	GR VB TB	GR VB TB	GR VB TB	GR VB TB	GR VB TB	GR VB TB	GR VB TB	GR VB TB	GR VB TB
SiO_2	54.34	54.38	47.65	48.37	52.43	48.28	48.59	47.08	50.78	50.43	50.56	49.91	52.75	52.87
TiO_2	0.91	1.14	1.53	1.56	1.43	1.55	1.59	1.53	1.41	1.24	1.32	1.86	1.32	1.39
Al_2O_3	17.21	16.13	16.48	17.56	15.61	15.99	16.50	17.24	15.10	16.34	15.59	15.72	15.39	15.05
Fe_2O_3	0.08	1.00	3.59	9.63	5.49	3.73	5.08	6.34	6.54	9.10	7.51	8.74	8.53	5.09
FeO	5.99	4.14	6.10	n.d.	3.14	5.21	4.18	3.63	2.84	nd	1.86	1.39	nd	3.11
MnO	0.11	0.08	0.15	0.15	0.09	0.17	0.17	0.18	0.13	0.13	0.14	0.07	0.12	0.11
MgO	7.77	8.17	6.70	6.22	6.21	6.38	5.67	5.14	6.88	7.33	6.95	6.53	7.10	7.18
CaO	7.59	5.45	11.21	10.39	8.83	11.53	10.73	12.11	10.11	9.83	9.95	6.53	7.06	6.78
Na_2O	2.02	1.26	3.33	3.43	3.94	3.89	4.15	3.55	3.59	3.40	3.52	3.86	3.56	3.22
K_2O	2.89	6.22	0.50	0.37	0.61	0.34	0.57	0.40	0.35	0.33	0.38	1.40	1.68	2.37
P_2O_5	0.25	0.30	0.13	0.24	0.21	0.17	0.19	0.20	0.18	0.17	0.18	0.31	0.20	0.28
L.O.I.	0.84	1.72	2.63	2.08	2.01	2.76	2.58	2.6	2.09	1.7	2.06	3.68	2.29	2.56
Total	100.00	99.99	100.00	100.00	100.00	100.00	100.00	100.00	100.00	100.00	100.02	100.00	100.00	100.01
mg#	72.15	76.62	59.21	59.23	60.86	60.11	56.73	52.70	61.47	64.43	61.98	58.81	65.18	65.39
V	173	144	231	254	244	242	251	238	209	203	210	260	209	199
Cr	417	606	167	175	140	161	165	213	201	222	226	93	173	223
Co	29.4	29.4	32.6	32.4	32.0	30.2	31.8	36.2	31.8	31.9	32.6	24.1	35.1	21.8
Ni	124	220	77.9	77.2	68.9	68.9	75.0	89.9	93.7	101	106	39.7	125	61.6
Rb	168	336	5.69	7.51	8.06	3.23	6.13	3.79	2.81	3.32	3.74	13.2	17.7	39.3
Sr	339	470	192	213	189	214	210	216	184	180	183	250	225	320
Ba	579	682	67	58.1	71.3	88.4	89.4	61.1	45.2	44.5	44.6	175	131	247
Cs	9.46	5.5	0.27	0.26	0.3	0.28	n.d	n.d.	0.24	0.31	0.3	0.51	1.00	3.80
Y	22.6	24.6	27.6	29.5	26.6	29.6	28.3	27.0	22.9	22.1	22.9	27.6	23.0	20.8
Zr	216	477	106	105	101	114	115	104	91.3	88.3	89.0	109	84.1	112
Hf	5.48	13.5	2.61	2.69	2.56	2.98	3.1	2.62	2.26	2.25	2.07	2.82	2.08	2.74
Nb	11.7	26.4	5.42	5.39	5.19	5.41	5.5	4.82	4.24	3.95	3.99	7.15	5.09	7.53
Ta	0.95	2.00	0.45	0.45	0.42	0.44	0.47	0.39	0.35	0.32	0.34	0.62	0.41	0.69
La	41.4	88.4	5.76	5.84	6.01	7.87	8.08	6.37	5.47	5.48	5.52	13.4	8.58	16.0
Ce	92.6	197	15.3	15.0	15.8	19.4	19.1	16.2	14	14.4	14.2	28.1	18.9	32.5
Pr	11.1	26.0	2.26	2.24	2.25	2.76	2.71	2.39	1.96	2.06	2.09	3.74	2.69	3.96
Nd	43.6	99.8	11.2	11.2	11.0	12.3	12.3	11.5	9.76	9.85	10.4	16.1	12.1	16.6
Sm	7.66	15.3	3.4	3.46	3.15	3.81	3.69	3.48	2.78	3.05	2.98	3.99	2.9	3.50
Eu	1.75	2.37	1.22	1.22	1.16	1.23	1.22	1.24	1.02	1.05	1.1	1.27	1.05	1.08
Gd	5.81	8.71	4.18	4.22	3.92	4.17	4.19	4.19	3.24	3.42	3.64	3.96	3.41	3.38
Tb	0.81	1.11	0.68	0.67	0.68	0.7	0.71	0.67	0.56	0.56	0.58	0.72	0.57	0.50
Dy	4.16	5.25	4.46	4.36	4.26	4.51	4.48	4.27	3.64	3.79	3.74	4.49	3.8	3.42
Ho	0.75	0.79	0.98	0.98	0.94	1.02	1.07	0.94	0.83	0.8	0.83	0.95	0.78	0.67
Er	2.12	2.37	2.64	2.66	2.59	2.92	2.9	2.59	2.24	2.22	2.26	2.59	2.15	1.85
Tm	0.31	0.26	0.43	0.42	0.44	0.47	0.46	0.41	0.37	0.36	0.36	0.41	0.35	0.31
Yb	1.97	2.00	2.77	2.88	2.76	2.94	2.86	2.65	2.29	2.37	2.31	2.69	2.20	2.04
Lu	0.32	0.30	0.44	0.44	0.42	0.47	0.44	0.43	0.36	0.36	0.36	0.42	0.33	0.28
Pb	25.0	40.0	1.74	1.64	1.72	3.81	3.58	2.2	1.88	1.64	1.83	6.47	2.74	9.93
U	4.62	9.91	0.19	0.47	0.26	0.28	0.34	0.43	0.24	0.2	0.22	1.12	0.56	3.46
Th	24.7	61.8	0.78	0.76	0.72	1.6	1.52	0.97	0.82	0.75	0.72	3.76	1.76	8.34

[a]Major element concentrations (wt.%) were determined by XRF at the facility of University of Pisa and trace element concentrations (ppm) by ICP-MS in Nancy [*Govindaraju*, 1989]. Ferrous/ferric iron ratios were determined by titration. For the Tyrrhenian Basin, major element concentrations are from *Beccaluva et al.* [1990]. A = Acquaforte, N = Nibbio, L = Latera, M = Montefiascone, MM = Monte Maggiore, B = Bracciano, SS = S. Sosio, SG = S. Giuliano, C = Castello, CP = Cava delle Piagge, GR = Gortani Ridge, VB = Vavilov Basin, RMP = Roman Magmatic Province, TMP = Tuscan Magmatic Province, TB = Tyrrhenian Basin.

highly potassic series (HKS) consists of strongly undersaturated volcanic rocks with ubiquitous leucite ranging from tephrites to phonolites. Ultrapotassic olivine-bearing leucitites and kalsilite-bearing melilites (kamafugites) and minettes have also been described from the RMP [*Holm and Munksgaard*, 1982; *Serri et al.*, 1993]. Despite these differences between the Tuscan and Roman Magmatic Provinces, recent geochemical and petrological studies of the RMP and TMP [*Peccerillo*, 1999; *Serri et al.*, 1993] have shown that the discrepancies between their respective magmatic products are not as distinctive as previously thought.

A2. Central and Southern Tyrrhenian Area: Vesuvius, Tyrrhenian Basin, Aeolian Islands, Iblean Basin, and Etna

[39] Quaternary magmatism in the central and southern Tyrrhenian area took place in both extension-related (Tyrrhenian Basin: 4–1.7 Ma [*Beccaluva et al.*, 1990; *Spadini et al.*, 1995]; Iblean Basin and Etna: 10–0 Ma [*Calanchi et al.*, 1989]) and subduction-related settings (Vesuvius: 0.25 Ma–1944 [*Barberi et al.*, 1981]; and Aeolian Islands: 1.3 Ma–present [*Beccaluva et al.*, 1985]).

[40] Vesuvius is a stratovolcano located a few kilometers southeast of Naples in the Campania region and is part of an older volcanic complex known as Somma–Vesuvius. A wide spectrum of eruptive patterns, from cinder cones and lava flows to catastrophic Plinian eruptions, characterizes its activity since at least 0.25 Ma. These volcanic events produced silica-undersaturated and K-rich lavas and pyroclastics that show variable compositions from tephrites to leucitites [*Ayuso et al.*, 1998; *Belkin et al.*, 1993; *Caprarelli et al.*, 1993; *Santacroce*, 1983; *Villemant et al.*, 1993]. The most recent eruptive period (1631–1944), to which our samples belong (1944), consists of predominantly effusive outcrops of pahoehoe and aa lavas that range from pyroxene- or leucite-bearing phonolitic to tephritic leucitites [*Belkin et al.*, 1993]. Because of its ultrapotassic affinity and enriched isotopic signatures, most authors consider the Vesuvius volcanic activity as belonging to the RMP [*D'Antonio et al.*, 1996; *Rogers et al.*, 1985; *Serri et al.*, 1993].

[41] The Tyrrhenian Basin is divided by the 41°N discontinuity (the Ortona–Roccamonfina line [*Patacca et al.*, 1992]) into a northern and a southern part, which are characterized by different directions and rates of extension. In the northern part rifting and thinning took place entirely within a continental environment, whereas in the southern part oceanic crust and seamount formation have developed fully. The southern part is in turn divided into two subbasins, Vavilov (4–3.5 Ma) and Marsili (1.9–1.7 Ma) [*Kastens and Mascle*, 1990; *Savelli*, 1988], believed to reflect a back arc setting with magmas varying in composition from transitional MORB (Sites 655, 373: ODP Leg 107) to calc-alkaline and high-K calc-alkaline (Sites 650, 651: ODP Leg 107 [*Beccaluva et al.*, 1990; *Bertrand et al.*, 1990; *Bonatti et al.*, 1990]). In addition, two seamounts (Magnaghi and Vavilov) in the Vavilov subbasin and the lower part of the Marsili seamount in the Marsili subbasin show typical OIB signatures.

[42] The Aeolian archipelago consists of seven volcanic islands that form an arc-shaped structure close to the Sicilian coast. The Aeolian volcanic rocks belong to distinct magmatic series that range from calc-alkaline to high-K calc-alkaline and are of shoshonitic to potassic affinity [*Barberi et al.*, 1973, 1974, 1994; *Ellam et al.*, 1988; *Francalanci and Manetti*, 1994]. They display distinct isotopic and trace element systematics consisting of a general increase in Sr and Pb isotope compositions and LILE contents from the west (Alicudi and Filicudi from where our samples originate) to the northeast (Vulcano, Lipari, Salina, Panarea, and Stromboli).

[43] The Iblean volcanic plateau covers a large area in the southeastern corner of Sicily and is the result predominantly of fissure activity that started in the Upper Triassic. Plio-Pleistocene magmatism (3–2 Ma [*Esperança and Crisci*, 1995]) produced little differentiated volcanics of sodic alkaline and subalkaline affinity (ranging from quartz-tholeiites to nephelinites) having geochemical features similar to those observed for within-plate sodic magmas. Incompatible trace element patterns and Sr and Nd isotope compositions of Quaternary volcanism of the Iblean area resemble those of HIMU [*Beccaluva et al.*, 1998].

[44] Etna is located along the east coast of Sicily. It is a Quaternary composite volcano that developed during several distinct stages, each consisting of lava flows and pyroclastics. Whereas the oldest magmatic activity (0.6 Ma [*Romano*, 1983]) is of tholeiitic affinity, the more recent magmatic products are of sodic alkaline affinity (0.22 Ma–present [*Armienti et al.*, 1989; *D'Orazio*, 1994; *Gillot et al.*, 1994]).

[45] **Acknowledgments.** We thank P. Télouk for assistance with the P54, P. Armienti, M. D'Orazio, G. Ferrara, L. Francalanci, A. Gioncada, P. Marianelli, A. Sbrana, and S. Tonarini for providing samples, and S. Conticelli and M. Murtas for help with sample collection. Financial support by the Institut National des Sciences de l'Univers, Cofinanziamento MURST, and the University of Pisa is gratefully acknowledged. We thank Al Hofmann, Bruce Nelson, Geoff Nowell, and an anonymous reviewer for careful and insightful reviews that significantly improved the manuscript.

References

Abouchami, W., S. J. G. Galer, and A. W. Hofmann, High precision lead isotope systematics of lavas from the Hawaiian Scientific Drilling Project, *Chem. Geol.*, *169*, 187–209, 2000.

Albarède, F., *Introduction to Geochemical Modeling*, 543 pp., Cambridge Univ. Press, New York, 1995.

Albarède, F., A. Simonetti, J. D. Vervoort, J. Blichert-Toft, and W. Abouchami, A Hf–Nd isotopic correlation in ferromanganese nodules, *Geophys. Res. Lett.*, *25*, 3895–3898, 1998.

Argnani, A., and C. Savelli, Cenozoic volcanism and tectonics in the southern Tyrrhenian sea: Space–time distribution and geodynamic significance, *Geodynamics*, *27*, 409–432, 1999.

Armienti, P., F. Innocenti, R. Petrini, M. Pompilio, and L. Villari, Petrology and Sr–Nd isotope geochemistry of recent lavas from Mt. Etna: Bearing on the volcano feeding system, *J. Volcanol. Geotherm. Res.*, *39*, 315–327, 1989.

Ayuso, R. A., B. De Vivo, G. Rolandi, R. R. Seal II, and A. Paone, Geochemical and isotopic (Nd–Pb–Sr–O) variations bearing on the genesis of volcanic rocks from Vesuvius Italy, *J. Volcanol. Geotherm. Res.*, *82*, 53–78, 1998.

Barberi, F., P. Gasparini, F. Innocenti, and L. Villari, Volcanism of the Southern Tyrrhenian Sea and its geodynamics implications, *J. Geophys. Res.*, *78*, 5221–5232, 1973.

Barberi, F., F. Innocenti, G. Ferrara, J. Keller, and L. Villari, Evolution of Eolian arc volcanism (Southern Tyrrhenian Sea), *Earth Planet. Sci. Lett.*, *21*, 269–276, 1974.

Barberi, F., H. Bizouard, R. Clocchiatti, N. Metrich, R. Santacroce, and A. Sbrana, The Somma–Vesuvius magma chamber; a petrological and volcanological approach, *Bull. Volcanol.*, *44*, 295–315, 1981.

Barberi, F., et al., Evoluzione stratigrafico-strutturale e vulcanismo Plio-Quaternario dell'area tosco-laziale, in *Evoluzione dei bacini neogenici e loro rapporti con il magmatismo Plio-Quaternario dell'area tosco-laziale*, pp. 7–9, Atti del Workshop, Pisa, Italy, 1991.

Barberi, F., A. Gandino, A. Gioncada, P. La Torre, A. Sbrana, and C. Zenucchini, The deep structure of the Eolian arc (Filicudi–Panarea–Vulcano sector) in light of gravity, magnetic and volcanological data, *J. Volcanol. Geotherm. Res.*, *61*, 189–206, 1994.

Bartole, R., The North Tyrrhenian–Northern Apennines post collisional system: Constraints for a geodynamical model, *Terra Nova*, *7*, 7–30, 1995.

Beccaluva, L., P. Di Girolamo, and G. Serri, High-K calc-alkalic, shoshonitic and leucititic volcanism of Campania (Roman Province, southern Italy): Trace element constraints on the genesis of an orogenic volcanism in a post-collisional extensional setting, in *Science Assembly: Potassic Volcanism—Etna Volcano*, edited by IAVCEI, Springer-Verlag, New York, 1985.

Beccaluva, L., et al., Geochemistry and mineralogy of volcanic rocks from ODP sites 650, 651, 655 and 654 in the Tyrrhenian Sea, in *Proceedings of the Ocean Drilling Program, Scientific Results*, edited by N. J. Stewart, pp. 49–73, U.S. Govt. Print. Off., Washington, D. C., 1990.

Beccaluva, L., P. Di Girolamo, and G. Serri, Petrogenesis and tectonic setting of the Roman Volcanic Province Italy, *Lithos*, *26*, 191–221, 1991.

Beccaluva, L., M. Coltorti, R. Galassi, G. Macciotta, and F. Siena, The Cainozoic calcalkaline magmatism of the western Mediterranean and its geodynamic significance, *Bol. Geofis. Teor. Appl.*, *141–144*, 293–308, 1994.

Beccaluva, L., F. Siena, M. Coltorti, A. Di Grande, A. Lo Giudice, G. Macciotta, R. Tassinari, and C. Vaccaro, Nephelinitic to tholeiitic magma generation in a transtensional tectonic setting: An integrated model for the Iblean volcanism, Sicily, *J. Petrol.*, *39*, 1547–1576, 1998.

Belkin, H. E., C. R. J. Kilburn, and B. De Vivo, *Chemistry of the Lavas and Tephra From the Recent (A.D. 1631–1944) Vesuvius (Italy) Volcanic Activity*, 44 pp., U.S. Geol. Surv., Reston, Va., 1993.

Bellon, H., Chronologie radiométric (K–Ar) des manifestations magmatique autour de la Mediterranée Occidentale entre 33 et 1 Ma, in *Sedimentary Basin of Mediterranean Margins*, edited by F. C. Wezel, pp. 341–368, Tectonoprint, Bologna, 1981.

Ben Othman, D., W. M. White, and J. Patchett, The geochemistry of marine sediments, island arc magma genesis, and crust–mantle recycling, *Earth Planet. Sci. Lett.*, *94*, 1–21, 1989.

Bergman, S. C., Lamproites and other potassium-rich igneous rocks: A review of their occurrence, mineralogy and geochemistry, in *Alkaline Igneous Rocks*, *Geol. Soc. Spec. Publ.*, edited by J. G. Fitton and B. G. J. Upton, pp. 103–189, 1987.

Bertrand, H., P. Boiven, and C. Robin, Geochemistry and mineralogy of volcanic rocks from ODP sites 650, 651, 655 and 654 in the Tyrrhenian Sea, in *Proceedings of the Ocean Drilling Program, Scientific Results*, edited by N. J. Stewart, pp. 75–92, U.S. Govt. Print. Off., Washington, D. C., 1990.

Blichert-Toft, J., C. Chauvel, and F. Albarède, Separation of Hf and Lu for high-precision isotope analysis of rock samples by magnetic sector-multiple collector ICP-MS, *Contrib. Mineral. Petrol.*, *127*, 248–260, 1997.

Blichert-Toft, J., F. A. Frey, and F. Albarède, Hf isotope evidence for pelagic sediments in the source of Hawaiian basalts, *Science*, *285*, 879–882, 1999a.

Blichert-Toft, J., J. D. Gleason, P. Télouk, and F. Albarède, The Lu–Hf isotope geochemistry of shergottites and the evolution of the Martian mantle–crust system, *Earth Planet. Sci. Lett.*, *173*, 25–39, 1999b.

Bonatti, E., M. Seyler, J. E. T. Channell, J. Giraudeau, and J. Mascle, Peridotites drilled from the Tyrrhenian Sea, O.D.P. Leg 107, in *Proceedings of the Ocean Drilling Program, Scientific Results*, edited by N. J. Stewart, pp. 37–47, U.S. Govt. Print. Off., Washington, D. C., 1990.

Calanchi, N., P. Colantoni, P. L. Rossi, M. Saitta, and G. Serri, The strait of Sicily continental rift system: Physiography and petrochemistry of the submarine volcanic centres, *Mar. Geol.*, *87*, 55–83, 1989.

Caprarelli, G., and B. De Vivo, Preliminary Sr and Nd isotopic data for recent lavas from Vesuvius volcano, *J. Volcanol. Geotherm. Res.*, *58*, 377–381, 1993.

Chase, C., Ocean island Pb: Two stages histories and mantle evolution, *Earth Planet. Sci. Lett.*, *52*, 277–284, 1981.

Chauvel, C., and J. Blichert-Toft, A hafnium isotope and trace element perspective on melting of the depleted mantle, *Earth Planet. Sci. Lett.*, *190*, 137–151, 2001.

Chauvel, C., A. W. Hofmann, and P. Vidal, HIMU–EM: The French Polynesian connection, *Earth Planet. Sci. Lett.*, *110*, 99–119, 1992.

Cioni, R., M. A. Laurenzi, A. Sbrana, and I. M. Villa, $^{40}Ar/^{39}Ar$ chronostratigraphy of the initial activity in the Sabatini volcanic complex (Italy), *Bol. Soc. Geol. Ital.*, *112*, 251–263, 1993.

Civetta, L., G. Orsi, P. Scandone, and R. Pece, Eastward migration of the Tuscan anatectic magmatism due to anticlockwise rotation of the Apennines, *Nature*, *276*, 604–606, 1978.

Civetta, L., F. Innocenti, P. Manetti, A. Peccerillo, and G. Poli, Geochemical characteristics of potassic volcanics from Mts Ernici (southern Latium, Italy), *Contrib. Mineral. Petrol.*, *78*, 37–47, 1981.

Civetta, L., G. Orsi, and A. Peccerillo, Petrogenesis of Na-alkaline rocks in back-arc areas; evidence from Ustica Island, southern Tyrrhenian Sea, in *Continental Magmatism*, edited by N. M. B.o.M.a.M. Resources, p. 52, Bur. of Mines and Mineral Prov., Socorro, N. M., 1989.

Class, C., and S. L. Goldstein, Plume–lithosphere interactions in the ocean basins: Constraints from the source mineralogy, *Earth Planet. Sci. Lett.*, *150*, 245–260, 1997.

Clocchiatti, R., A. Del Moro, A. Gioncada, J. L. Joron, M. Mosbah, L. Pinarelli, and A. Sbrana, Assessment of a shallow magmatic system; the 1888–1890 eruption Volcano Island, Italy, *Bull. Volcanol.*, *56*, 466–486, 1994.

Conticelli, S., The effect of crustal contamination on ultrapotassic magmas with lamproitic affinity: Mineralogical, geochemical and isotope data from Torre Alfina and xenoliths, central Italy, *Chem. Geol.*, *149*, 51–81, 1998.

Cundari, A., Role of subduction in the genesis of leucite-bearing rocks: Facts or fashion? Reply to A. D. Edgar's discussion paper, *Contrib. Mineral. Petrol.*, *73*, 432–434, 1980.

D'Antonio, M., G. R. Tilton, and L. Civetta, Petrogenesis of Italian alkaline lavas deduced from Pb–Sr–Nd isotope relationships, in *Earth Processes: Reading the Isotopic Code*, edited by A. Basu and S. Hart, pp. 253–267, AGU, Washington, D. C., 1996.

D'Orazio, M., Natura ed evoluzione delle vulcaniti dell'Etna e loro relazioni con il magmatismo Ibleo, Unpublished Ph.D. thesis, Università di Pisa, Pisa, Italy, 1994.

D'Orazio, M., S. Tonarini, F. Innocenti, and M. Pompilio, Northern Valle del Bove volcanic succession (Mt. Etna, Sicily): Petrography, geochemistry and Sr–Nd data, *Acta Vulcanol.*, *9*, 73–86, 1997.

Del Moro, A., A. Gioncada, L. Pinarelli, A. Sbrana, and J. L. Joron, Sr, Nd, and Pb isotope evidence for open system evolution at Vulcano Aeolian Arc, Italy, *Lithos*, *43*, 81–106, 1998.

Deniel, C., Geochemical and isotopic (Sr–Nd–Pb) evidence for plume lithosphere interactions in the genesis of Grande Comore magmas (Indian Ocean), *Chem. Geol.*, *144*, 281–333, 1998.

Doglioni, C., P. Harabaglia, S. Merlini, F. Mongelli, A. Peccerillo, and C. Piromallo, Orogens and slabs vs. their direction of subduction, *Earth Sci. Rev.*, *45*, 167–208, 1999.

Ellam, R. M., M. A. Menzies, C. J. Hawkesworth, W. P. Leeman, M. Rosi, and G. Serri, The transition from calk-alkaline to potassic orogenic magmatism in the Aeolian Islands, Southern Italy, *Volcanology*, *50*, 386–398, 1988.

Ellam, R. M., C. J. Hawkesworth, M. A. Menzies, and N. W. Rogers, The volcanism of Southern Italy: Role of subduction and the relationship between potassic and sodic alkaline magmatism, *J. Geophys. Res.*, *94*, 4589–4601, 1989.

Esperança, S., and G. Crisci, The island of Pantelleria: A case for the development of DMM–HIMU isotopic compositions in a long-lived extensional setting, *Earth Planet. Sci. Lett.*, *136*, 167–182, 1995.

Ferrara, G., O. Giuliani, S. Tonarini, and I.M. Villa, Datability and isotopic disequilibrium in anatectic volcanites from S. Vincenzo and Tolfa (Tuscany—Latium), *Rend. Soc. Ital. Mineral. Petrol.*, *7*, 72, 1988.

Ferrara, G., R. Petrini, G. Serri, and S. Tonarini, Petrology and isotope-geochemistry of San Vincenzo rhyolites (Tuscany Italy), *Bull. Volcanol.*, *51*, 379–388, 1989.

Fisk, M. R., B. G. J. Upton, C. E. Ford, and W. M. White, Geochemical and experimental study of the genesis of Reunion Island Indian Ocean, *J. Geophys. Res.*, *93*, 4933–4950, 1988.

Fleck, R.J., and R. E. Criss, Strontium and oxygen isotopic variations in Mesozoic and Tertiary plutons of Central Idaho, *Contrib. Mineral. Petrol.*, *90*, 291–308, 1985.

Foley, S. F., G. Venturelli, D. H. Green, and L. Toscani, The ultrapotassic rocks; characteristics, classification, and constraints for petrogenetic models, *Earth Sci. Rev.*, *24*, 81–134, 1987.

Fornaseri, M., Geochronology of volcanic rocks from Latium and from Umbria, *Rend. Soc. Ital. Min. Petrol.*, *40*, 73–106, 1985.

Francalanci, L., and P. Manetti, Geodynamic models of the southern Tyrrhenian region: Constraints from the petrology and geochemistry of the Aeolian volcanic rocks, *Bol. Geofis. Teor. Appl.*, *36*, 283–292, 1994.

Francalanci, L., S. R. Taylor, M. T. McCulloch, and J. D. Woodhead, Geochemical and isotopic variations in the calc-alkaline rocks of Aeolian arc, southern Tyrrhenian Sea, Italy: Constraints on magma genesis, *Contrib. Mineral. Petrol.*, *113*, 300–313, 1993.

Gasperini, D., J. Blichert-Toft, D. Bosch, A. Del Moro, P. Macera, P. Telouk, and F. Albarède, Evidence from Sardinian basalt geochemistry for recycling of plume heads into the Earth's mantle, *Nature*, *408*, 701–704, 2000.

Gillot, P. Y., G. Kieffer, and R. Romano, The evolution of the Mount Etna in the light of potassium–argon dating, *Acta Vulcanol.*, *5*, 81–87, 1994.

Giunchi, C., R. Sabadini, E. Boschi, and P. Gasperini, Dynamic models of subduction: Geophysical and geological evidence in the Tyrrhenian Sea, *Geophys. J. Int.*, *126*, 555–578, 1996.

Govindaraju, K., compilation of working values and sample description for 272 geostandards, *Geostand. Newsl.*, *13*, 113, 1989.

Graham, D., J. Lupton, F. Albarède, and M. Condomines, A 360,000 year helium isotope record from Piton de la Fournaise Réunion Island, *Nature*, *347*, 545–548, 1990.

Hamelin, B., B. Lambret, J. L. Joron, M. Treuil, and C. J. Allègre, Geochemistry of basalts from the Tyrrhenian Sea, *Nature*, *278*, 832–834, 1979.

Hanan, B. B., and D. W. Graham, Lead and helium isotope evidence from oceanic basalts for a common deep source of mantle plumes, *Science*, *272*, 991–995, 1996.

Hart, S. R., D. C. Gerlach, and W. M. White, A possible new Sr–Nd–Pb mantle array and consequences for mantle mixing, *Geochim. Cosmochim. Acta*, *50*, 1551–1557, 1986.

Hart, S. R., E. H. Hauri, L. A. Oschmann, and J. A. Whitehead, Mantle plumes and entrainment: Isotopic evidence, *Science*, *256*, 517–520, 1992.

Hawkesworth, C. J., and R. Vollmer, Crustal contamination versus enriched mantle: $^{143}Nd/^{144}Nd$ and $^{87}Sr/^{86}Sr$ evidence from the Italian volcanics, *Contrib. Mineral. Petrol.*, *69*, 151–165, 1979.

Hawkesworth, C. J., P. D. Kempton, N. W. Rogers, and R. M. Ellam, Continental mantle lithosphere, and shallow level enrichment processes in the Earth's mantle, *Earth Planet. Sci. Lett.*, *96*, 256–268, 1990.

Hickey, R. L., F. A. Frey, and D. C. Gerlach, Multiple sources for basaltic arc rocks from the southern volcanic zone of the Andes (34–41°S): Trace element and isotopic evidence for contributions from subducted oceanic crust, mantle and continental crust, *J. Geophys. Res.*, *91*, 5963–5983, 1986.

Hofmann, A. W., Chemical differentiation of the Earth: The relationship between mantle, continental crust, and oceanic crust, *Earth Planet. Sci. Lett.*, *90*, 297–314, 1988.

Hofmann, A. W., Mantle geochemistry: The message from oceanic volcanism, *Nature*, *385*, 219–229, 1997.

Hofmann, A. W., and W. M. White, Mantle plumes from ancient oceanic crust, *Earth Planet. Sci. Lett.*, *57*, 421–436, 1982.

Holm, P. M., and N. C. Munksgaard, Evidence for mantle metasomatism: An oxygen and strontium isotope study of the Vulsinian district Central Italy, *Earth Planet. Sci. Lett.*, *60*, 376–388, 1982.

Innocenti, F., G. Serri, G. Ferrara, P. Manetti, and S. Tonarini, Genesis and classifications of the rocks of the Tuscan Magmatic Province: Thirty years after Marinelli's model, *Acta Vulcanol.*, *2*, 247–265, 1992.

Jochum, K. P., A. W. Hofmann, E. Ito, H. M. Seufert, and W. M. White, K, U and Th in mid-ocean ridge basalt glasses and heat production, K/U and K/Rb in the mantle, *Nature*, *306*, 431–436, 1983.

Juteau, M., A. Michard, and F. Albarède, The Pb–Sr–Nd isotope geochemistry of some recent circum-Mediterranean granites, *Contrib. Mineral. Petrol.*, *92*, 331–340, 1986.

Kamenetsky, V., N. Métrich, and R. Cioni, Potassic primary melts of Vulsini (Roman Province): Evidence from mineralogy and melt inclusions, *Contrib. Mineral. Petrol.*, *120*, 186–196, 1995.

Kastens, K., and J. Mascle, The geological evolution of the Tyrrhenian Sea; an introduction to the scientific results of ODP Leg 107, in *Proceedings of the Ocean Drilling Program, Scientific Results*, edited by N. J. Stewart, pp. 3–26, U.S. Govt. Print. Off., Washington, D. C., 1990.

Laurenzi, M. A., and I. M. Villa, $^{40}Ar/^{39}Ar$ chronostratigraphy of Vico ignimbrites, *Per. Mineral.*, *56*, 285–293, 1987.

Lavecchia, G., and F. Stoppa, Distribuzione regionale dei litotipi ignei, traccianti geochimici ed altri aspetti caratteristici dell'area tirrenica e peritirrenica. Sua evoluzione tettonica e verifica del modello estensionale, in *Studi Geologici Camerti*, edited by D. S. d. T. Università degli Studi di Camerino, pp. 413–428, AGIP–CNR–ENEL, Camerino, Italy, 1991.

Liotta, D., L. Cernobori, and R. Nicolich, Restricted rifting and its coexistence with compressional structures; results from the CROP 3 traverse (Northern Apennines Italy), *Terra Nova*, *10*, 16–20, 1998.

Lombardi, G., M. Nicoletti, and C. Petrucciani, Età delle vulcaniti acide del complesso Tolfetano Cerite e Manziate (Lazio nord-occidentale), *Per. Mineral.*, *43*, 351–376, 1974.

Manhes, G., J. F. Minster, and C. J. Allègre, Comparative uranium–thorium–lead and rubidium–strontium study of the Saint Severin amphoterite: Consequences for early solar system chronology, *Earth Planet. Sci. Lett.*, *39*, 14–24, 1978.

Maréchal, C. N., P. Télouk, and F. Albarède, Precise analysis of copper and zinc isotopic compositions by plasma-source mass spectrometry, *Chem. Geol.*, *156*, 251–273, 1999.

Marinelli, G., Magma evolution in Italy, in *Geology of Italy*, edited by C. H. Squyres, pp. 165–219, Earth Sci. Soc. of the Libian Arab. Repub., Tripoli, L.A.R., 1975.

Marinelli, G., and M. Mittempergher, On the genesis of some magmas of typical Mediterranean (potassic) suite, *Bull. Volcanol.*, *29*, 113–140, 1966.

McKenzie, D., and R. K. O'Nions, Mantle reservoirs and oceanic island basalts, *Nature*, *301*, 229–231, 1983.

Meletti, C., E. Patacca, and P. Scandone, Construction of a seismotectonic model: The case of Italy, *Pure Appl. Geophys.*, *157*, 11–35, 2000.

Morris, J. D., and S. R. Hart, Isotopic and incompatible element constraints on the genesis of island arc volcanics from Cold Bay and Amak Island, Aleutians, and implications for mantle structure, *Geochim. Cosmochim. Acta*, *47*, 2015–2030, 1983.

Patacca, E., R. Sartori, and P. Scandone, Tyrrhenian basin and Apenninic arcs: Kinematic relations since Late Tortonian times, *Mem. Soc. Geol. Ital.*, *45*, 425–451, 1992.

Patchett, P. J., W. M. White, H. Feldmann, S. Kielinczuk, and A. W. Hofmann, Hafnium/rare earth element fractionation in the sedimentary system and crustal recycling into the Earth's mantle, *Earth Planet. Sci. Lett.*, *69*, 365–378, 1984.

Peccerillo, A., Relationships between ultrapotassic and carbonate-rich volcanic rocks in central Italy: Petrogenetic and geodynamic implications, *Lithos*, *43*, 267–279, 1998.

Peccerillo, A., Multiple mantle metasomatism in central–southern Italy: Geochemical effects, timing and geodynamic implications, *Geology*, *27*, 315–317, 1999.

Peccerillo, A., and P. Manetti, The potassium alkaline volcanism of Central–Southern Italy: A review of the data relevant to petrogenesis and geodynamic significance, *Trans. Geol. Soc. S. Africa*, *88*, 379–394, 1985.

Peccerillo, A., and P. Manetti, Petrological characteristics and the genesis of the recent magmatism of southern Tuscany and northern Latium, *Per. Mineral.*, *56*, 157–172, 1987.

Plank, T., and C. H. Langmuir, The chemical composition of subducting sediment and its consequences for the crust and mantle, *Chem. Geol.*, *145*, 325–394, 1998.

Rogers, N. W., C. J. Hawkesworth, R. J. Parker, and J. S. Marsh, The geochemistry of potassic lavas from Vulsini, central Italy, and implications for mantle enrich ment processes beneath the Roman Region, *Contrib. Mineral. Petrol.*, *90*, 244–257, 1985.

Romano, R., Succession of the volcanic activity in the Etnean area, *Mem. Soc. Geol. It.*, *23*, 27–28, 1983.

Rudnick, R. L., and D. M. Fountain, Nature and composition of the continental crust: A lower crustal perspective, *Rev. Geophys.*, *33*, 267–309, 1995.

Santacroce, R., A general model for the behavior of the Somma–Vesuvius volcanic complex, *J. Volcanol. Geotherm. Res.*, *17*, 237–248, 1983.

Savelli, C., Late Oligocene to Recent episodes of magmatism in and around the Tyrrhenian Sea; implications for the processes of opening in a young inter-arc basin of intra-orogenic (Mediterranean) type, *Tectonophysics*, *146*, 163–181, 1988.

Schiano, P., R. Clocchiatti, L. Ottolini, and T. Busa, Transition of Mount Etna lavas from a mantle-plume to an island-arc magmatic source, *Nature*, *412*, 900–904, 2001.

Schilling, J.-G., R. H. Kingsley, B. B. Hanan, and B. L. McCully, Nd–Sr–Pb isotopic variations along the Gulf of Aden: Evidence for Afar mantle plume–continental lithosphere interaction, *J. Geophys. Res.*, *97*, 10,927–10,966, 1992.

Serri, G., Neogene–Quaternary magmatic activity and its geodynamic implications in the Central Mediterranean region, *Ann. Geofis.*, *40*(3), 681–703, 1997.

Serri, G., F. Innocenti, P. Manetti, S. Tonarini, and G. Ferrara, Il magmatismo Neogenico–Quaternario dell'area tosco-laziale-umbra: implicazioni sui modelli di evoluzione geodinamica dell'Appennino Settentrionale, in *Studi Geologici Camerti*, edited by D.S.d.T. Università degli Studi di Camerino, pp. 429–463, AGIP–CNR–ENEL, 1991.

Serri, G., F. Innocenti, and P. Manetti, Geochemical and petrological evidence of the subduction of delaminated Adriatic continental lithosphere in the genesis of the Neogene–Quaternary magmatism of central Italy, *Tectonophysics*, *223*, 117–147, 1993.

Sobolev, A. V., and M. Chaussidon, H2O concentrations in primary melts from supra-subduction zones and mid-ocean ridges: Implications for H_2O storage and recycling in the mantle, *Earth Planet. Sci. Lett.*, *137*, 45–55, 1996.

Spadini, G., G. Bertotti, and S. Cloeting, Tectono-stratigraphic modeling of the Sardinian margin of the Tyrrhenian Sea, *Tectonophysics*, *252*, 269–284, 1975.

Stacey, J. S., and J. D. Kramers, Approximation of terrestrial lead isotope evolution by a two-stage model, *Earth Planet. Sci. Lett.*, *26*, 207–221, 1975.

Sun, S. S., Lead isotopic study of young volcanic rocks from mid-ocean ridges, ocean islands and island arcs, in *The Evidence for Chemical Heterogeneity in the Earth's Mantle*, pp. 409–445, R. Soc. of London, London, 1980.

Tamburelli, C., D. Babbucci, and E. Mantovani, Geodynamic implications of "subduction-related" magmatism: Insights from the Tyrrhenian-Apennines region, *J. Volcanol. Geotherm. Res.*, *104*, 33–43, 2000.

Taylor, S. R., and S. M. McLennan, The geochemical evolution of the continental crust, *Rev. Geophys.*, *33*, 241–265, 1995.

Thompson, R. N., Primary basalts and magma genesis. Alban Hills, Roman Comagmatic Province Central Italy, *Contrib. Mineral. Petrol.*, *50*, 91–108, 1977.

Thompson, R. N., M. A. Morrison, G. L. Hendry, and S. J. Parry, An assessment of the relative roles of the crust and mantle in magma genesis: An elemental approach, *Philos. Trans. R. Soc. London, Ser. A*, *310*, 549–590, 1984.

Thorpe, R. S., P. W. Francis, and L. O'Callaghan, Relative roles of source composition, fractional crystallization and crustal contamination in the petrogenesis of Andean volcanic rocks, *Philos. Trans. R. Soc. London, Ser. A*, *310*, 675–692, 1984.

Todt, W., R. A. Cliff, A. Hanser, and A. W. Hofmann, *Evaluation of a ^{202}Pb–^{205}Pb double spike for high-precision lead isotope analysis*, in *Earth Processes: Reading the Isotopic Code*, edited by A. Basu and S. Hart, pp. 429–437, AGU, Washington, D. C., 1996.

Tonarini, S., M. D'Orazio, P. Armienti, F. Innocenti, and V. Scribano, Geochemical features of eastern Sicily lithosphere as probed by Hyblean xenoliths and lavas, *Eur. J. Mineral.*, *8*, 1153–1173, 1996.

Turi, B., and H. P. J. Taylor, Oxygen isotope studies of potassic volcanic rocks of the Roman Province, central Italy, *Contrib. Mineral. Petrol.*, *55*, 1–31, 1976.

Vervoort, J. D., P. J. Patchett, J. Blichert-Toft, and F. Albarède, Relationships between Lu–Hf and Sm–Nd isotopic systems in the global sedimentary system, *Earth Planet. Sci. Lett.*, *168*, 79–99, 1999.

Vervoort, J. D., P. J. Patchett, F. Albarède, J. Blichert-Toft, R. L. Rudnick, and H. Downes, Hf–Nd isotopic evolution of the lower crust, *Earth Planet. Sci. Lett.*, *181*, 115–129, 2000.

Vidal, P., C. Chauvel, and R. Brousse, Large mantle heterogeneity beneath French Polynesia, *Nature*, *307*, 536–538, 1984.

Villemant, B., B. Trigila, and B. De Vivo, Geochemistry of Vesuvius volcanics during 1631–1944 period, *J. Volcanol. Geotherm. Res.*, *58*, 291–313, 1993.

Vollmer, R., Rb–Sr and U–Th–Pb systematics of alkaline rocks: The alkaline rocks from Italy, *Geochim. Cosmochim. Acta*, *40*, 283–295, 1976.

Vollmer, R., and C. J. Hawkesworth, Lead isotopic composition of the potassic rocks from Roccamonfina (South Italy), *Earth Planet. Sci. Lett.*, *47*, 91–101, 1980.

Westaway, R., Seismic moment summation for historical earthquakes in Italy: Tectonic implications, *J. Geophys. Res.*, *97*, 15,437–15,464, 1992.

White, W. M., and R. A. Duncan, Geochemistry and geochronology of the Society Islands: New evidence for deep mantle recycling, in *Earth Processes: Reading the Isotopic Code*, edited by A. Basu and S. Hart, pp. 183–206, AGU, Washington, D. C., 1996.

White, W. M., and A. W. Hofmann, Sr and Nd isotope geochemistry of oceanic basalts and mantle evolution, *Nature*, *296*, 821–825, 1982.

White, W. M., and J. Patchett, Hf–Nd–Sr isotopes and incompatible element abundances in island arcs: Implications for magma origins and crust–mantle evolution, *Earth Planet. Sci. Lett.*, *67*, 167–185, 1984.

White, W. M., F. Albarède, and P. Télouk, High-precision analysis of Pb isotopic ratios using multi-collector ICP-MS, *Chem. Geol.*, *167*, 257–270, 2000.

Wilson, M., *Igneous Petrogenesis*, 466 pp., Chapman and Hall, New York, 1989.

Wortel, M. J. R., and W. Spakman, Subduction and slab detachment in the Mediterranean–Carpathian region, *Science*, *290*, 1910–1917, 2000.

F. Albarède, J. Blichert-Toft, and D. Gasperini, Ecole Normale Supérieure, 46, Allee d'Italie, 69364, Lyon, Cedex 07, France. (d.gasperini@dst.unipi.it)

D. Bosch, Université Montpellier 2, 22, Place E. Bataillon, 34095, Montpellier, Cedex 05, France.

A. Del Moro, Istituto di Geocronologia e Geochimica Isotopica, CNR, Via Alfieri, 1, 56010, Ghezzano-Pisa, Italy.

P. Macera, Dipartimento di Scienze della Terra, Universita' degli Studi di Pisa, Via S. Maria, 53, 56126, Pisa, Italy.